2024 年 11 月 地 球 学 报 Nov. 2024
第 45 卷 第 6 期: 854-870 Acta Geoscientica Sinica Vol.45 No.6: 854-870
www.cagsbulletin.com

# 青藏高原大型地震断裂带的变形机制

张 蕾[1,2], 李海兵[1,2]*, 王 焕[1,2], 吴 琼[3], 杨少华[1,2], 孙知明[4], 司家亮[1,2], Marie-Luce CHEVALIER[1,2], 曹 勇[4], 郑 勇[1,2], 潘家伟[1,2], 刘栋梁[1,2], 赵中宝[1,2], 马绪宣[1,2], 卢海建[1,2]

1)中国地质科学院地质研究所, 自然资源部大陆动力学重点实验室, 北京 100037;
2)江苏东海大陆深孔地壳活动国家野外科学观测研究站, 江苏连云港 222300;
3)北京石油机械有限公司, 北京 102206;
4)中国地质科学院地质力学研究所, 自然资源部古地磁与古构造重建重点实验室, 北京 100081

**摘 要:** 近年来, 大震频发, 地震发生机制和地震断裂作用的研究已成为当今社会的重大课题, 而断裂带的变形机制, 尤其是大型地震断裂带的变形机制是认识断裂活动性和地震发生机制的关键。本文通过介绍青藏高原东缘龙门山断裂带和鲜水河断裂带的最新研究成果, 探讨青藏高原大型地震断裂带的变形机制, 主要认识如下: (1)汶川地震使不同性质断层同时破裂, 并在地壳浅部(~732.6 m 深度)富流体断层泥中发生了熔融作用, 颠覆了地震的传统认识, 深化了对浅部断层力学性质的认识。(2)龙门山断裂带映秀—北川断裂带在晚三叠世曾经发生 M*w*7.4~7.9 级的逆冲-左行走滑大地震, 断裂岩的高磁化率各向异性度值指示了大地震活动。(3)汶川—茂县断裂带在新生代时期存在三期不同构造变形, 青藏高原东缘不存在下地壳隧道流模式。(4)龙门山断裂带汶川—茂县断裂带曾经发生了摩擦热温度>500 ℃的大地震活动, 孕震环境为还原性的含有硫化物的低温热液流体环境。(5)强震频发的鲜水河断裂带是藏东南物质外迁的主要边界, 具有长期蠕滑变形行为, 流体作用较强, 流体的注入明显提高断层核部强矿物含量, 促进了蠕滑断层的局部变强。上述认识丰富和完善了断裂作用理论, 提高了对青藏高原大型地震断裂带变形机制的认识, 为断裂带活动性、地震发生机制、地震危险性评估和防震减灾提供了科学依据。

**关键词:** 断裂岩; 变形机制; 龙门山断裂带; 鲜水河断裂带; 青藏高原

**中图分类号:** P315.2 **文献标志码:** A **doi:** 10.3975/cagsb.2024.102801

# Deformation Mechanism of Large Earthquake Fault Zone in the Tibetan Plateau

ZHANG Lei[1,2], LI Haibing[1,2]*, WANG Huan[1,2], WU Qiong[3], YANG Shaohua[1,2], SUN Zhiming[4], SI Jialiang[1,2], Marie-Luce CHEVALIER[1,2], CAO Yong[4], ZHENG Yong[1,2], PAN Jiawei[1,2], LIU Dongliang[1,2], ZHAO Zhongbao[1,2], MA Xuxuan[1,2], LU Haijian[1,2]

1) *MNR Key Laboratory of Continental Dynamics*, *Institute of Geology*, *Chinese Academy of Geological Sciences*, *Beijing* 100037;
2) *Jiangsu Donghai Continental Deep Borehole Crustal Activity National Observation and Research Station*, *Lianyungang*, *Jiangsu* 222300;
3) *Beijing Petroleum Machinery Co.*, *Ltd*, *Beijing* 102206;
4) *MNR Key Laboratory of Paleomagnetism and Tectonic Reconstruction*, *Institute of Geomechanics*, *Chinese Academy of Geological Sciences*, *Beijing* 100081

**Abstract:** Recently, large earthquakes have occurred frequently, and earthquake mechanism and earthquake

本文由国家自然科学基金项目(编号: 42230312; 42172262; 42372266; 42072240; 42020104007; 42272270; 42374121)、中国地质科学院基本科研业务费项目(编号: J2403)和中国地质调查局地质调查项目(编号: DD20221630)联合资助。获中国地质科学院 2023 年度十大科技进展第三名。
收稿日期: 2024-08-01; 改回日期: 2024-10-17; 网络首发日期: 2024-10-29。责任编辑: 马铭株。
第一作者简介: 张蕾, 女, 1988 年生。博士, 副研究员。主要从事岩石磁学与断裂作用研究工作。E-mail: zhanglei881102@126.com。
*通信作者: 李海兵, 男, 1966 年生。博士, 研究员。主要从事构造地质学及活动构造研究。E-mail: lihaibing06@163.com。

faulting have become important topics in society. The deformation mechanism of fault zones, especially large earthquake fault zones, is the key to understanding fault activity and earthquake mechanisms. The aim of this study was to discuss the deformation mechanism of the large earthquake fault zone in the Tibetan Plateau by analyzing recent research on the Longmen Shan and Xianshuihe fault zones in the eastern Tibetan Plateau. The results are as follows: (1) The Wenchuan earthquake simultaneously ruptured on different faults and formed a pseudotachylyte vein at an extremely shallow depth (~732.6 m), which was generated in an unconsolidated, fluid-rich fault gouge. This finding overturns our traditional understanding of earthquakes and deepens our understanding of the mechanical properties of shallow faults. (2) A Late Triassic M*w*~7.4 to 7.9 earthquake had occurred along the Yingxiu–Beichuan fault, Longmen Shan fault zone, and the focal mechanism of this large magnitude earthquake was left-lateral, strike-slip motion. The high degree of magnetic anisotropy in the fault rocks is an indication of a high-strain seismogenic environment and a new important indicator of large earthquakes. (3) Three deformation phases were identified in the Wenhuan–Maoxian fault zone during the Cenozoic, in contrast to the predictions of the lower crustal channel-flow extrusion models. (4) Large earthquakes with high frictional heating (>500 °C) have occurred along the Wenhuan–Maoxian fault zone in the past, and the seismogenic environment was a reductive environment with low-temperature hydrothermal fluids. (5) The Xianshuihe fault system is the main boundary for the outward migration of material in southeastern Tibet. The Xianshuihe fault zone, with frequent large earthquakes, exhibits long-term creep deformation behavior. The fluid influx increases the content of strong minerals within the fault core, thereby locally strengthening the creeping fault. These results enrich and improve the faulting theory, improve our understanding of the deformation mechanism of large earthquake fault zones in the Tibetan Plateau, and provide a scientific basis for fault-zone activity, earthquake mechanisms, earthquake risk assessment, and earthquake prevention and reduction.

**Key words:** fault rocks; deformation mechanism; Longmen Shan fault zone; Xianshuihe fault zone; Tibetan Plateau

2001 年 M*s*8.1 昆仑地震拉开了全球大地震频繁发生的序幕(Zhang, 2013), 随后发生了 2004 年 *M*w9.3 苏门答腊地震、2008 年 *M*w7.9 汶川地震、2010 年 *M*w8.8 智利地震、2011 年 *M*w9.0 日本宫城地震、2015 年 *M*w8.0 尼泊尔地震和 2018 年 *M*w7.9 阿拉斯加地震等大地震活动。大陆内部地震灾害已经造成了大量人员伤亡和财产损失(Zhang, 2013)。因此, 地震发生机制和地震断裂作用的研究已经成为当今社会的重大课题。断裂带变形机制是认识断裂作用和地震发生机制的关键。

龙门山断裂带和鲜水河断裂带是青藏高原东缘的大型重要地震断裂带(图 1), 是世界上陆内变形最强烈的地区之一, 具有全球地貌高程最陡、地震最为频发、地质灾害最为严重的特点, 是大陆内部断裂带深部过程与浅表响应表现最为显著的地区。龙门山断裂带是一条经常发生大地震的活动断裂带, 是我国重要的强震危险区域, 该断裂带上类似汶川地震的大地震复发周期为 3 000~6 000 a (Shen et al., 2009)。2008 年汶川大地震之后, 龙门山断裂带已经成为地学研究的热点区域(徐锡伟等, 2008; 李海兵等, 2008; 许志琴等, 2008; 王二七等, 2008; 张培震等, 2008; 李勇等, 2009; Jia et al., 2010; Fu et al., 2011; Wang et al., 2015, 2019a; Zhang et al., 2017, 2018)。鲜水河断裂带不仅是控制青藏高原物质向东及南东方向挤出的北部边界, 而且是高应变速率带(Wang et al., 2020)。鲜水河断裂带强震频发, 是中国乃至世界上陆内活动性最强的断裂带之一(Allen et al., 1991; 闻学泽, 2000; Wen et al., 2008; Bai et al., 2018, 2021)。自 1725 年以来已发生 17 次 *M*s>6 的大地震, 包括 2010 年玉树 *M*s7.1 级地震和 1833 年嵩明 *M*s8.0 级大地震(国家地震局震害防御司, 1995; 中国地震局震害防御司, 1999; USGS, 2020), 平均 36 年就会发生一次类似汶川地震的大地震。鲜水河断裂带的库伦应力在汶川地震之后急剧增加(Toda et al., 2008; Shen et al., 2009; Yang et al., 2015), 导致该断裂带在未来发生大地震的概率变大。2014 年康定地区 *M*s5.9 级和 *M*s5.6 级两次地震事件及 2022 年 *M*s6.8 级泸定地震不足以释放整条断裂带上的巨大应力, 因此, 鲜水河断裂带仍有发生强震的危险。龙门山断裂带和鲜水河断裂带是中国大陆陆内重要的地震断裂带。龙门山断裂带以逆冲运动为主(李勇等, 2006; Hubbard et al., 2009), 鲜水河断裂带是以走滑运动为主(闻学泽等, 1989; Klinger, 2010; Zielke et al., 2015); 龙门山断裂带大地震复发周期长而鲜水河断裂带大地震复发周期短。因此, 对比分析青藏高原东缘两条运动性质不同断裂带的变形机制对于认识大陆内部地震发生机制具有重要意义。

本文通过介绍龙门山断裂带和鲜水河断裂带的最新研究成果, 对比分析两条断裂带的断裂岩组

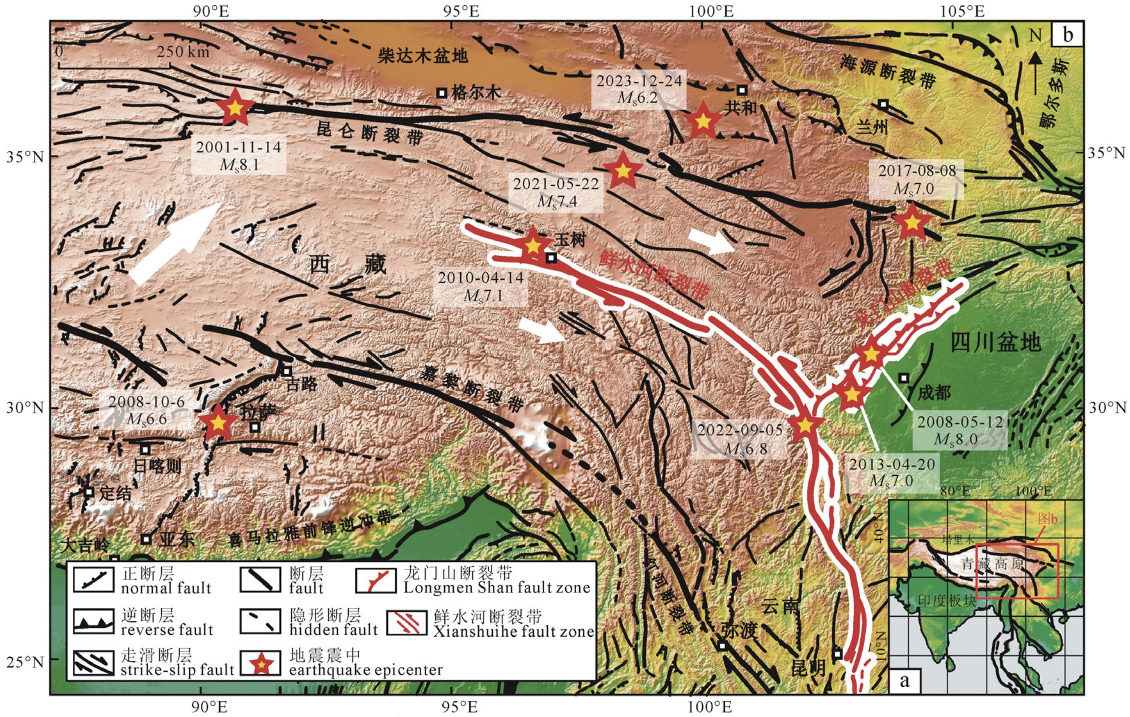


**图 1 青藏高原构造略图(a)和青藏高原东部及邻区主要大型活动断裂带分布图(b)**

**Fig. 1 Tectonic map of the Tibetan Plateau (a) and distribution of large active fault zones in the eastern Tibetan Plateau (b)**

成及结构特征、地震机制及孕震环境等，进一步探讨青藏高原大型断裂带的变形机制。

## 1 龙门山断裂带

### 1.1 大地震在浅部含水断层泥中形成的熔融作用

与断层作用相关的假玄武玻璃(又称作假熔岩，是凝固的摩擦熔融体)被喻为“地震化石”，是大地震滑动的重要标志(Sibson, 1975; Cowan, 1999)，记录了地震断层滑动过程中物理-化学和力学属性等重要信息，是认识大地震形成环境和发生机制的重要物质(Lin, 2008)。大量研究认为假玄武玻璃形成于断层深部(深度>4 km)孕震带(Sibson, 1977; Fialko et al., 2005; 图 2)，并且只能形成于弱流体作用的坚硬干岩石中(Sibson et al., 2006)。法国科西嘉岛的假玄武玻璃形成于地幔(Andersen et al., 2006)，日本 Nojima 断裂中的假玄武玻璃的形成深度>15 km(Boullier et al., 2001)，新西兰奥塔戈的假玄武玻璃形成深度是~6~12 km(Barker, 2005)，意大利南阿尔卑斯山的假玄武玻璃的形成深度是9~11 km(Mittempergher et al., 2014)。龙门山断裂带八角庙露头的假玄武玻璃形成深度为10~14 km(Zheng et al., 2016)，WFSD-2 钻孔岩心的假玄武玻璃形成于<15 km 的深度处(张蕾等, 2018)。自然界中也发现了一些形成深度较浅的假玄武玻璃，例如美国内华达州出露的假玄武玻璃形成深度是~2~6 km(Kirkpatrick et al., 2012)，格陵兰岛的假玄武玻璃形成深度~1.6 km(Maddock et al., 1987)。但是浅部存在的大量孔隙流体在断层滑动过程中产生热增压作用，从而增加断层滑动带中的流体压力并降低了有效正应力，进而抑制了同震摩擦热温度的升高(Rice, 2006; Brantut et al., 2010)。因此，浅部断层泥熔融自然形成假玄武玻璃尚未有过报道。

Wang et al.(2023)在汶川地震断裂带科学钻探 1 号钻孔(WFSD-1)岩心深度 732.6 m 处发现了一层新鲜的假玄武玻璃，其围岩是未固结且流体作用较强的断层泥(图 3, 4a~b)。该假玄武玻璃中的碎块主要是石英，基质的主要成分是长石和黏土矿物熔融的非晶质(图 4e)。基质中可见流动构造，并发育大量不规则的微裂隙(图 4e~g)。基质富集 Ba 元素，且被重晶石($BaSO_4$)小细脉切割，指示了发震及震后的流体作用。龙门山断裂带八角庙露头(Wang et al., 2015)和 WFSD-2 钻孔岩心(Zhang et al., 2017)中发现古地震形成的假玄武玻璃同样含有石英碎块以及长石、黏土矿物熔融的非晶质，但是微裂隙较少。Zhang et al.(2021)对 WFSD-2 钻孔岩心假玄武玻璃的围岩碎裂岩进行高温加热实验发现新生熔体在降温过程中会形成大量未被其他物质填充的微裂隙。假玄武玻璃在流体作用下可能会发生蚀变(Kirkpatrick et al., 2013; Fondriest et al., 2020)，而 WFSD-1 岩心 732.6 m 深度处的假玄武玻璃未发生蚀变，表明其可能是最近一次大地震的产物。龙门山断裂带大地震复发周期为 3 000~6 000 a(Shen et al., 2009)，因此，新发现的假玄武玻璃可能是 2008 年汶川大地震的产物(Wang et al., 2023)。WFSD-1 钻孔

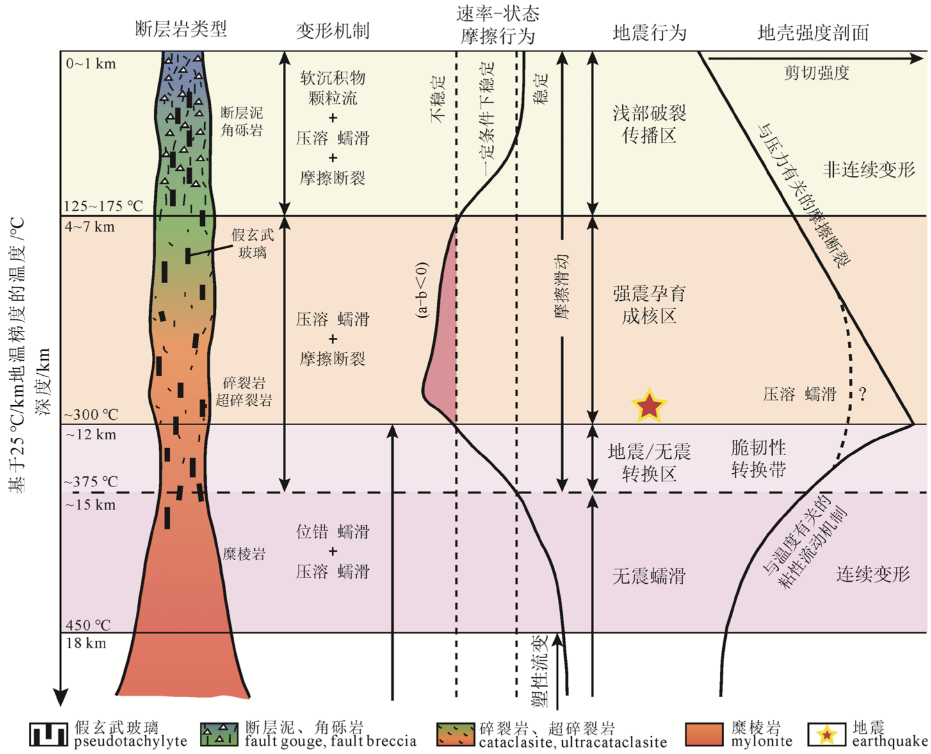

图 2　深大剪切带的地质和地震特征的模型图(据 Sibson, 1983; Scholz, 1988 修改)

Fig. 2　A synoptic shear zone model with the important geological and seismological features (modified from Sibson, 1983; Scholz, 1988)

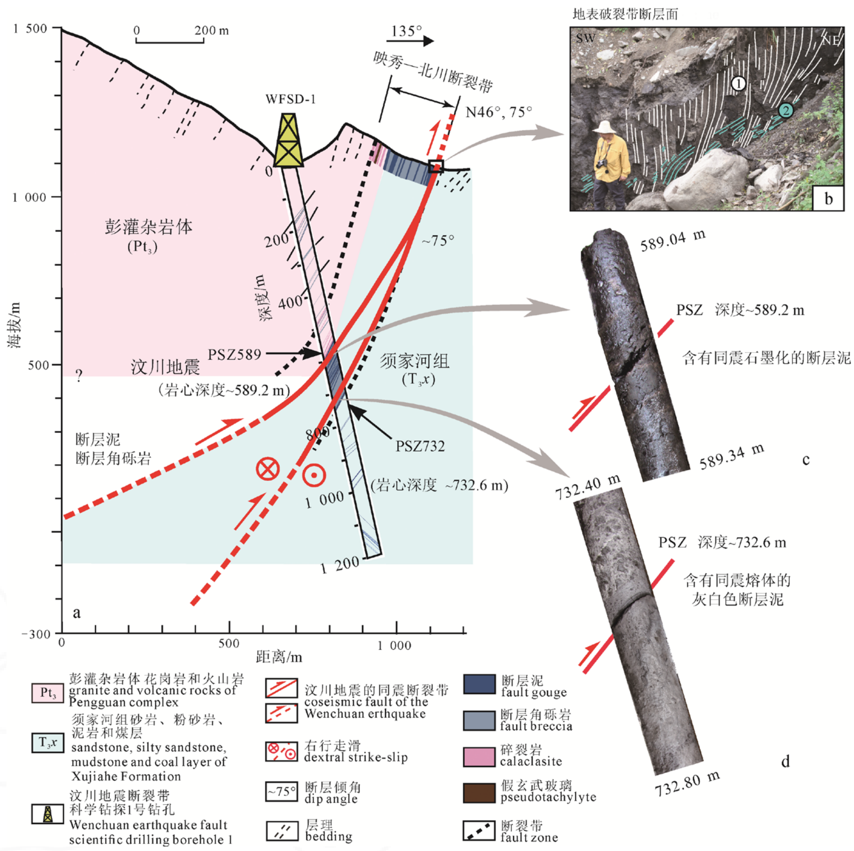

a—穿过 WFSD-1 钻孔的地质剖面; b—汶川地震同震地表破裂带，破裂面上可见两组擦痕; c—589.04~589.34 m 深处岩心特征，其中包含主滑动带 PSZ589(断层泥石墨化作用); d—732.40~732.80 m 深处岩心特征，包含形成假玄武玻璃的主滑动带 PSZ732(摩擦熔融机制)。

a–geological cross-section across the WFSD-1; b–surface rupture near the WFSD-1 drill site, and two sets of striae decorate the fault surface; c–drill core from 589.04 m to 589.34 m, including the graphite-rich PSZ589 (black gouge with graphitization); d–drill core from 732.40 m to 732.80 m, including the pseudotachylyte-bearing PSZ732 (frictional melting).

图 3　WFSD-1 岩心中两条汶川地震主滑动带(Wang et al., 2023)

Fig. 3　Two principal slip zones of the Wenchuan earthquake in WFSD-1 core (Wang et al., 2023)

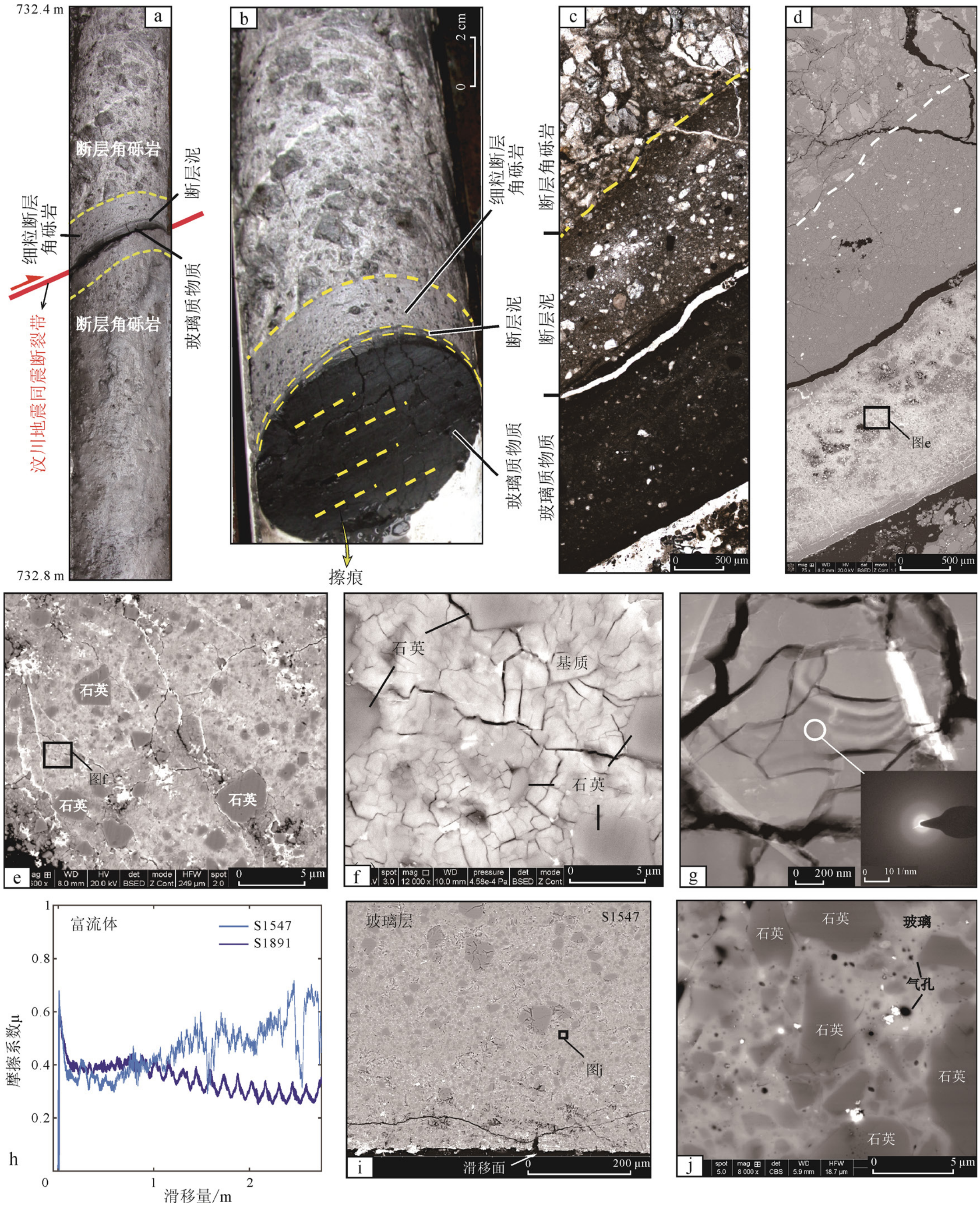


a—WFSD-1 钻孔 732.4~732.8 m 深度的岩心照片，包含了厚约 2 mm 的黑色假玄武玻璃；b—含假玄武玻璃的岩心特征，在假玄武玻璃表面可见擦痕和镜面构造；c—主滑移面的显微结构特征，从上到下依次为断层角砾岩、断层泥和假玄武玻璃；d—扫描电镜下主滑移面的结构特征；e~g—假玄武玻璃基质中发育有众多不规则微裂隙和波纹状构造，同时衍射图样显示为非晶质物质；h—WFSD-1 断层泥高速摩擦实验数据：富流体条件下浅灰色断层泥摩擦系数与滑动位移量的关系；i~j—实验中形成的熔体的扫描电镜图像。

a–the core at a depth of 732.4–732.8 m, including a black 2-mm-thick pseudotachylyte layer; b–pseudotachylyte bound by a striated, mirror-like principal slip surface; c–optical microscopy image of the main slip zone; the slip zone consists of layers of fault breccia, fault gouge, and glass-like materials; d–backscattered electron-scanning electron microscopy image of the main slip zone; e–g–matrix including randomly oriented, open microcracks and glass-like matrix with a few tens-of-nanometers-thick ripples and microcracks (transmission electron microscopy image), inset showing diffraction patterns; h–high speed friction experimental data of WFSD-1 fault gouge; friction coefficient versus slip under fluid-rich conditions (metal holders); i–j–backscattered electron-scanning electron microscopy images of melt from frictional experiments.

**图 4 汶川地震熔体的结构特征和摩擦实验结果(Wang et al., 2023；王焕等, 2023)**

**Fig. 4 Structural characteristics of Wenchuan earthquake melt and results of friction experiments (Wang et al., 2023; WANG et al., 2023)**

岩心中断层泥高速摩擦试验结果证实在 732 m 深度处如果发生地震滑动会形成假玄武玻璃(Wang et al., 2023；王焕等, 2023；图 4h~j)。因此，WFSD-1 岩心 732.6 m 深处的假玄武玻璃是汶川地震的同震产物，指示了其所处位置是汶川地震的主滑动带。这是第一次发现浅层流体作用较强的断层泥摩擦熔融形成

的假玄武玻璃。结合先前在 WFSD-1 岩心 589.2 m 深处识别出的另一主滑动带(PSZ589; Li et al., 2013), Wang et al.(2023)认为大地震过程中断层可以沿多个分支同时产生破裂(图 3), 并且可以在浅部富流体的条件下发生摩擦熔融。地震破裂通常沿一条断层传播, 或者破裂从一条断层跳跃至另一条(分支)断层传播。然而, 汶川地震使不同性质断层同时破裂, 显示大地震断层破裂的复杂性, 为研究大地震发生机制和破裂传播提供新的思考。

通过对 WFSD-1 钻孔岩心假玄武玻璃的结构特征和摩擦实验结果的分析, Wang et al.(2023)认为地壳浅层流体作用较强的断层泥中可以发生同震摩擦熔融作用。地震摩擦热通常会引发粒间孔隙流体热膨胀增压, 形成同震断层弱化(热增压机制), 这一过程不利于摩擦熔融的发生(Di Toro et al., 2009)。断层在非常浅且富流体的位置发生摩擦熔融有助于对断层浅部力学属性和变形机制的全新认识。综合相关研究, 王焕等(2023)认为同震断裂摩擦熔融普遍存在于自然界中, 但是大部分浅部形成的假玄武玻璃却很少被保存或者识别, 原因是假玄武玻璃的结构和成分可能在后期的断裂作用、蚀变和脱玻化过程中发生改变。例如, Wang et al.(2019b)发现龙门山断裂带地表出露的假玄武玻璃和 WFSD-2 钻孔岩心中的假玄武玻璃化学性质存在明显的差别, 地表的假玄武玻璃经历了表生流体作用, 出现了含 Ca 元素的新生矿物并且 K 和 Ti 元素含量较低。此外, 龙门山断裂带地表出露的部分假玄武玻璃也可能因后期蚀变作用而导致非晶质特征不明显(Wang et al., 2015)。这一认识颠覆了假玄武玻璃在自然界中很难形成且只产生于干的环境下的传统认识。

### 1.2　映秀—北川断裂带晚三叠世古地震机制

断裂带应力作用控制着不同类型地震的发生, 决定了断裂带的变形机制, 因此, 认识断裂带应力特征是揭示大地震发生机制的重要内容(Andrews, 2002; Rice, 2006)。龙门山断裂带是我国重要的强震危险区域, 由于没有直接揭示原始强震应力信息的物质, 制约着龙门山断裂带强震机制和变形机制的认识。岩石磁组构可以用来确定断裂带应力和应变特征(Levi et al., 2006; Jayangondaperumal et al., 2010), 被称为磁学“应力计”(Yang et al., 2013)。地震成因假玄武玻璃和断层泥磁组构研究确定了古地震机制和古应力场特征(Ferré et al., 2015, 2016; Chou et al., 2020)。在龙门山断裂带映秀—北川断裂带八角庙露头出露了一组地震断裂熔融成因的假玄武玻璃脉体(图 5a)(Wang et al., 2015), 年代学研究表明其形成于晚三叠世(Zheng et al., 2016)。

假玄武玻璃脉体中可见石英蚀变边界、流动构造、针状和树根状微晶结构(Wang et al., 2015), 而假玄武玻璃围岩碎裂岩中的石英在 1 300 ℃高温时发生了部分熔融(Zhang et al., 2018, 2021), 表明该套假玄武玻璃是同震摩擦熔融的产物, 同震摩擦热温度高达 1 300 ℃。假玄武玻璃脉体包括断层脉和注入脉(图 5b, c), 脉体厚度平均为 1~2 cm, 根据 Sibson(1975) 的经验公式估算同震位移量为 4.4~17.4 m。根据 Wells et al.(1994)的经验公式估算对应的震级为 *M*w7.4~7.9(Zhang et al., 2024)。断层面走向是 N39°~68°, 倾向是 SE 向, 倾角为 74°~85°。假玄武玻璃注入脉与断层脉之间夹角较大, 注入脉主要分布在 T 剪切或 R1 方向上, 断层脉分布在 Y 剪切方向。假玄武玻璃脉体可见一组擦痕构造(图 5c~e), 倾伏向 S218°E, 倾伏角 10°(图 5f)。

Zhang et al.(2024)对映秀—北川断裂带八角庙假玄武玻璃、碎裂岩和初碎裂岩开展了磁组构测试, 结果显示假玄武玻璃具有较高的磁化率各项异性度 P 值, P 值平均值为 1.44, 最高值为 2.8。假玄武玻璃及其附近碎裂岩的 P 值远高于围岩和龙门山地区的沉积岩(罗良等, 2006, 2008, 2013; Luo et al., 2014; Zhou et al., 2023), 并且远高于世界上其他地震断裂带的假玄武玻璃, 如意大利阿尔卑斯山、中国台湾、法国科西嘉岛、美国加利福尼亚和苏格兰(Ferré et al., 2015, 2016), 以及中国台湾集集地震断裂带的断层泥(Chou et al., 2020)。假玄武玻璃高 P 值可能与龙门山断裂带强应变环境有关(Zhang et al., 2024), 类似的情况也在世界上其他断裂带上出现(Housen et al., 1995; Kontny et al., 2012; Merz et al., 2019)。断裂岩高 P 值是强应变地震发生环境的标志, 也是大地震的一个新的重要标志(Zhang et al., 2024)。龙门山断裂带围岩的 P 值通常小于 1.2(Li et al., 2007; 罗良等, 2006, 2008, 2013; Luo et al., 2014), 因此, 当断裂岩的 P 值大于 1.2 时, 即可证明地震发生在强应变环境下。

八角庙露头假玄武玻璃脉体表面的擦痕是同震构造, 地震机制图解揭示古地震机制是逆冲-左行走滑(图 5g)。由于假玄武玻璃组构只记录了后期的同震黏性剪切, 那么这些组构相对于剪切面/假玄武玻璃面往往是倾斜的。它们的夹角指示了准确的剪切方向, 为地震运动学提供了重要的信息(Ferré et al., 2015, 2016)。Ferré et al.(2015)首次提出可以用假玄武玻璃的磁组构揭示大地震机制, 并准确确定了意大利阿尔卑斯山西部的假玄武玻璃的同震地震机制是正断层。随后, Ferré et al.(2016)为了更加准确地测量假玄武玻璃脉体的磁组构, 提出采

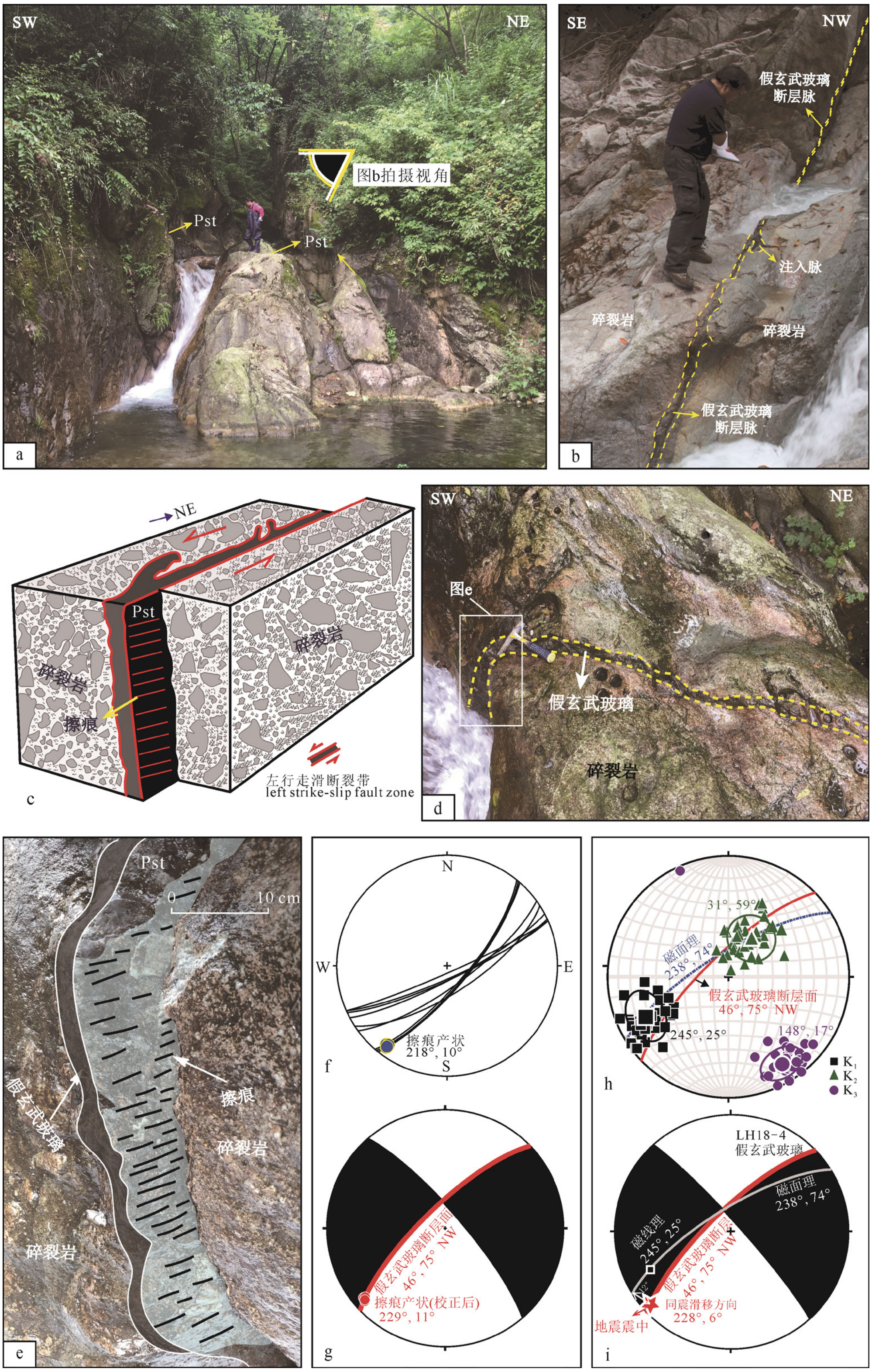


a—龙门山八角庙露头全景照片; b—假玄武玻璃脉体; c—假玄武玻璃脉体和碎裂岩模型; d—假玄武玻璃脉体和碎裂岩照片; e—假玄武玻璃脉体表面的擦痕照片及素描; f—断层面理和擦痕线理的投图; g—擦痕特征指示的地震机制图解; h—假玄武玻璃的磁组构结果, $K_1$—最大应变主轴, $K_2$—中间应变主轴, $K_3$—最小应变主轴; i—假玄武玻璃磁组构指示的地震机制图解。Pst—假玄武玻璃。

a–panoramic photograph of Bajiaomiao outcrop in the Longmen Shan fault zone; b–pseudotachylyte veins; c–model for pseudotachylyte veins and cataclasite; d–photograph of pseudotachylyte veins and cataclasite; e–photograph and sketch of striations of pseudotachylyte veins; f–polar stereographic projection of foliations and striations along the pseudotachylyte; g–earthquake focal mechanism diagram of a Late Triassic large earthquake revealed by striations along the pseudotachylyte; h–AMS directional parameters of pseudotachylyte, which are shown as trend and dip angles of $K_1$, $K_2$ and $K_3$ axes, $K_1$–maximum principal axis of strain, $K_2$–middle principal axis of strain, $K_3$–minimum principal axis of strain; i–earthquake focal mechanism diagram of a Late Triassic large earthquake revealed by the AMS results of pseudotachylyte. Pst–pseudotachylyte.

**图 5　龙门山断裂带假玄武玻璃磁组构和擦痕指示的运动学特征(Zhang et al., 2024)**

**Fig. 5　Magnetic fabric and kinematics features revealed by striations along the pseudotachylyte from the Longmen Shan fault zone (Zhang et al., 2024)**

集假玄武玻璃的 mini-AMS 样品(磁组构小样品, 边长约为 3.5 mm 的小立方体)进行磁组构测试, 并在科西嘉岛、加利福尼亚和苏格兰的假玄武玻璃中获得了较好的测试结果。假玄武玻璃的磁组构测试为龙门山地区古地震机制的研究提供了新思路。产状校正后, 八角庙露头假玄武玻璃磁组构揭示古大地震活动走向是~248°, 倾角为 38°。晚三叠世古大地震活动的地震机制是逆冲-左行走滑(图 5h, i), 并指示了 NNW 向主压应力方向。磁组构揭示的古大地震机制与假玄武玻璃表面擦痕(校正后)揭示的古大地震机制是一致的, 与 2008 年汶川地震机制不同。主压应力方向与现今主压应力方向不同。晚三叠世古大地震同震滑移量是 4.4~17.4 m, 对应的地震震级为 *M*w7.5~7.9, 与 2008 年汶川地震相似。以上结果表明龙门山构造带是一条具有继承性的活动断裂带, 持续的地震活动从晚三叠世左行走滑断裂转变为新生代右行走滑断裂, 发生转变的主要原因是主压应力场方向从 NNW 向转变为 NW 向。

### 1.3　汶川—茂县断裂带新生代构造变形特征

印度板块和欧亚板块碰撞形成了青藏高原极其复杂的内部结构(Yin et al., 2000; Tapponnier et al., 2001)。新生代以来, 青藏高原的演化过程主要有三种模式: 刚性块体挤出模式(Tapponnier et al., 2001)、下地壳隧道流模式(Royden et al., 1997, 2008)和逆冲断层形成的地壳水平缩短模式(Hubbard et al., 2009; Wang et al., 2019a)。其中下地壳隧道流模式是一个很重要的模式, 前人认为自~15 Ma(中新世中期)以来, 下地壳流向东转移导致青藏高原中部东西向伸展和东部地形向外迁移(Klemperer, 2006; Adams et al., 2022)。下地壳流在龙门山形成世界上最陡峭的大陆斜坡, 高出四川盆地近 5 000 m(Burchfiel et al., 2008; Royden et al., 2008), 龙门山断裂带成为下地壳隧道流模式造山的典型。也有学者提出逆冲断层促使地壳水平缩短、纵向增厚(Hubbard et al., 2009, 2010; Tian et al., 2013; Lu et al., 2016; Wang et al., 2019a)。两种模式下, 龙门山地区断裂活动呈现出不同的性质, 在下地壳隧道流模式下, 龙门山断裂带的后山断裂必须是正断层, 与具有逆冲断裂活动性质的前山断裂一起调节块体向上挤出(Royden et al., 2008; Burchfiel et al., 2008); 而地壳缩短模式下的后山断裂同样也得是逆冲断裂(Hubbard et al., 2009, 2010)。因此, 龙门山断裂带后山断裂汶川—茂县断裂带的运动学特征是区分上述两种模式的关键。

Ge et al.(2023)结合构造观察、断层泥 K/Ar 测年和云母 $^{40}Ar/^{39}Ar$ 测年, 确定了汶川—茂县断裂带新生代运动学特征。通过详细的野外调查和研究, 查明汶川—茂县断裂带存在宽约 3 km、向 NW 陡倾的韧性剪切带, 其内部发育由断层泥、断层角砾岩和破碎带组成的脆性断裂带, 宽度~50 m、向 NW 方向陡倾(60°~70°)。通过显微构造研究, 确定了韧性剪切带内部存在两期不同性质的韧性变形, 分别为向 NW 方向的正断下滑兼右行走滑变形和由 NW 向 SE 方向的逆冲变形。年代学研究将两期韧性变形时代限定在~28 Ma 和~15 Ma。绿泥石和石英晶格温度计指示变形温度分别为~350 ℃和~300 ℃。高精度遥感影像显示汶川—茂县断裂带在龙门山中部有着明显的线性分布, 断裂带中断层泥的宏观与微观构造显示(脆性)断裂具有明显右行走滑兼逆冲分量的变形。被错断的河流和地质单元指示右行走滑位移量为~25 km。另外, 断层泥中自生伊利石的测年结果限定脆性变形时代为~6 Ma, 计算断裂带右行走滑速率为~3.6 mm/a。断裂活动的直接测年结果(Ge et al., 2023)与前人热年代学数据对断裂活动所约束的间接时代较为吻合, 确定汶川—茂县断裂带在新生代存在三期构造变形阶段(图 6): 渐新世时期(~30~25 Ma)为正断兼右行走滑运动、渐新世到中新世时期(25~15 Ma)为逆冲运动和晚中新世时期(~6 Ma)为右行走滑伴随逆冲运动。汶川—茂县断裂未经历新生代纯下滑正断变形, 并且自渐新世以来主要存在水平缩短变形。结合区域地球物理资料, Ge et al.(2023)认为下地壳隧道流可能不是产生和维持龙门山陡峭地形的有效机制, 龙门山的形成是地壳水平缩短增厚的结果。这一研究揭示了新生代龙门山汶川—茂县断裂带的变形行为, 确定了汶川—茂县断裂带在新生代存在三期不同构造变形阶段, 为强震背景和山脉隆升机制提供了新证据。

### 1.4　汶川—茂县断裂带古地震孕震环境

汶川—茂县断裂带孕震和发震环境对认识龙门山断裂带变形行为和演化过程具有重要意义。张蕾等(2023)以汶川—茂县断裂带断层泥和断层角砾岩为研究对象, 分析其断裂作用环境, 为认识龙门山断裂带变形行为和地震发生机制提供重要的科学信息。汶川—茂县断裂带北部出露的断层角砾岩和断层泥的磁化率值高于围岩, 最大值分别是围岩的 15 倍和 30 倍。围岩的主要载磁矿物是大量顺磁性矿物以及少量磁黄铁矿和针铁矿。断层角砾岩的主要载磁矿物同样是顺磁性矿物以及磁黄铁矿和针铁矿, 而断层泥则是含有顺磁性矿物、磁铁矿、磁黄铁矿和针铁矿。围岩中顺磁性矿物在含有硫化物低温热液流体中生成了磁黄铁矿导致断层角砾岩高磁化率值, 而断层泥具有高磁化率值异常的原因可能是在地震摩擦热和流体作用下生成了磁铁矿, 并在低温热液作用下生成了磁黄铁矿(张蕾等, 2023)。

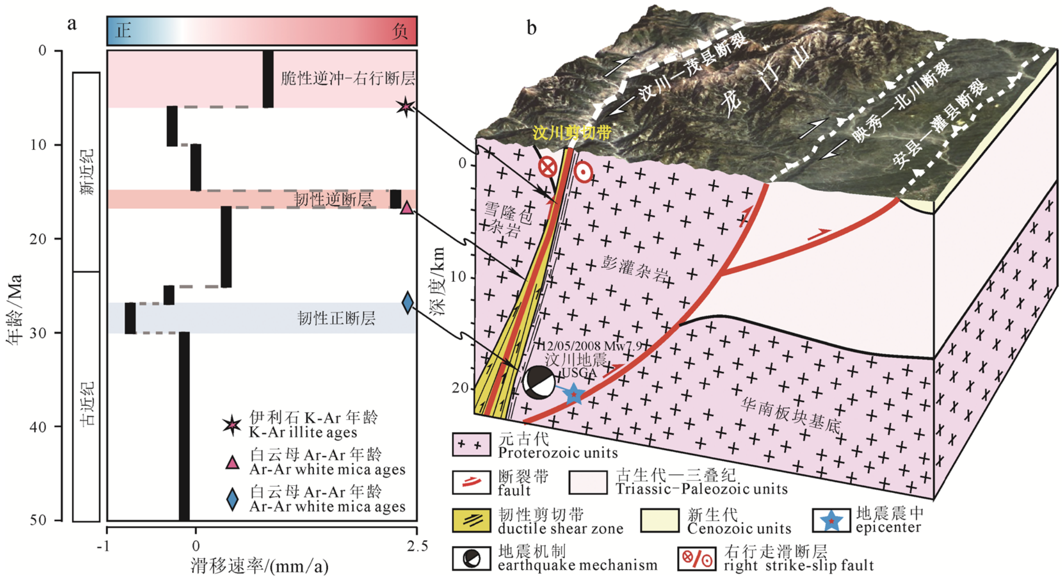

图 6 汶川—茂县断裂带的运动学特征(Ge et al., 2023)
Fig. 6 Kinematic characteristics of the Wenchuan–Maoxian fault zone (Ge et al., 2023)

地震过程中压力、温度、氧化还原环境和流体作用等环境因素的变化可以改变断裂岩的磁性特征，如磁性矿物的种类、颗粒大小、含量、剩磁方向和强度等(Hirono et al., 2006; Mishima et al., 2009; Chou et al., 2012; Ferré et al., 2012; Yang et al., 2020)。因此，地震断裂带磁性特征可以分析地震断裂作用中温度、流体、应力以及氧化还原性等特征(Chou et al., 2012; Ferré et al., 2012, 2015, 2016; 张蕾等, 2019, 2023; Yang et al., 2020; Zhang et al., 2024)。汶川—茂县断裂带断层泥高磁化率值异常和新生磁铁矿指示了该断裂带曾经发生大地震活动，同震摩擦热温度>500 ℃; 断层泥中新生磁黄铁矿指示了含有硫化物的还原性孕震和发震环境; 断层角砾岩含有新生磁黄铁矿及大量针铁矿表明大地震发生后经历了强还原性低温热液流体作用，并且其中含有硫化物(张蕾等, 2023)。该研究明确揭示了汶川—茂县断裂带上的古大地震活动，并确定了其孕震及发震环境，为龙门山断裂带地震发生机制和演化过程的研究提供了重要的科学数据。

## 2 鲜水河断裂带

### 2.1 鲜水河断裂带变形行为

鲜水河断裂带是中国大陆内部构造活动性最强的大型走滑断裂带，是世界上地震活动最强的断裂带之一(Allen et al., 1991; 闻学泽, 2000; Bai et al., 2018, 2021)。自 1725 年以来，鲜水河共发生过 9 次 6.9 级以上的大地震活动，破裂几乎遍布整条鲜水河断裂带(Wen et al., 2008; 潘家伟等, 2020)。大地震发生后，区域应力大量释放，断裂发生震后闭锁，降低了未来大地震危险性(闻学泽, 2000)。然而，自 2008 年 *M*s8.0 级汶川地震、2013 年 *M*s7.0 级芦山地震和 2017 年 *M*s7.0 级九寨沟地震之后，鲜水河断裂带库伦应力急增，未来强震危险性增大(Toda et al., 2008; Shan et al., 2009; Cheng et al., 2011; 徐晶等, 2013; Jiang et al., 2015; Guo et al., 2018)。20 世纪以来，巴颜喀拉地块周缘发生了 7 级以上的大地震共计 11 次，位于中段的鲜水河断裂带的地震危险性急剧增大。鲜水河断裂带变形行为和地震危险性的研究已经成为了地学界关注的重点。前人根据大地测量学研究和详细野外调查发现鲜水河断裂带具有广泛的非震蠕滑变形行为(Li et al., 2021; Qiao et al., 2021, 2022)，在 7.6~18.5 km 深度处闭锁(Qiao et al., 2021)。地学界普遍认为长期缓慢滑动、连续释放构造应力和伴随多微震的蠕滑断裂带通常不容易发生大地震(Sibson,1975; Gratier et al., 2013; Chen et al., 2017; Harris, 2017)。因此，鲜水河断裂带蠕滑行为特征与历史记录的大地震活动是不一致的，同时其长期变形行为尚不明确。为了理清鲜水河断裂带的长期变形行为，Wu et al.(2023)和吴琼等(2023)选取非震蠕滑和地震黏滑兼具的鲜水河断裂带乾宁段断裂岩为研究对象(图 7)，通过显微构造观察、矿物学和地球化学等分析，在蠕滑断层地震机制及流体作用等方面取得了新的重要认识。

研究剖面可见 700 m 宽的断裂岩带和 100 m 宽的砂岩破碎带，断裂岩带包括断层角砾岩和呈弥散性分布的薄层断层泥(图 7; 吴琼等, 2023)。断裂带内普遍可见压溶构造，表明鲜水河断裂带乾宁段内具有长期蠕滑变形行为。然而，断裂带局部断裂岩具有快速滑动特征，比如宽 2 m 的局部滑移带内大小不均一的棱角状碎块杂乱分布，同时可见断层楔

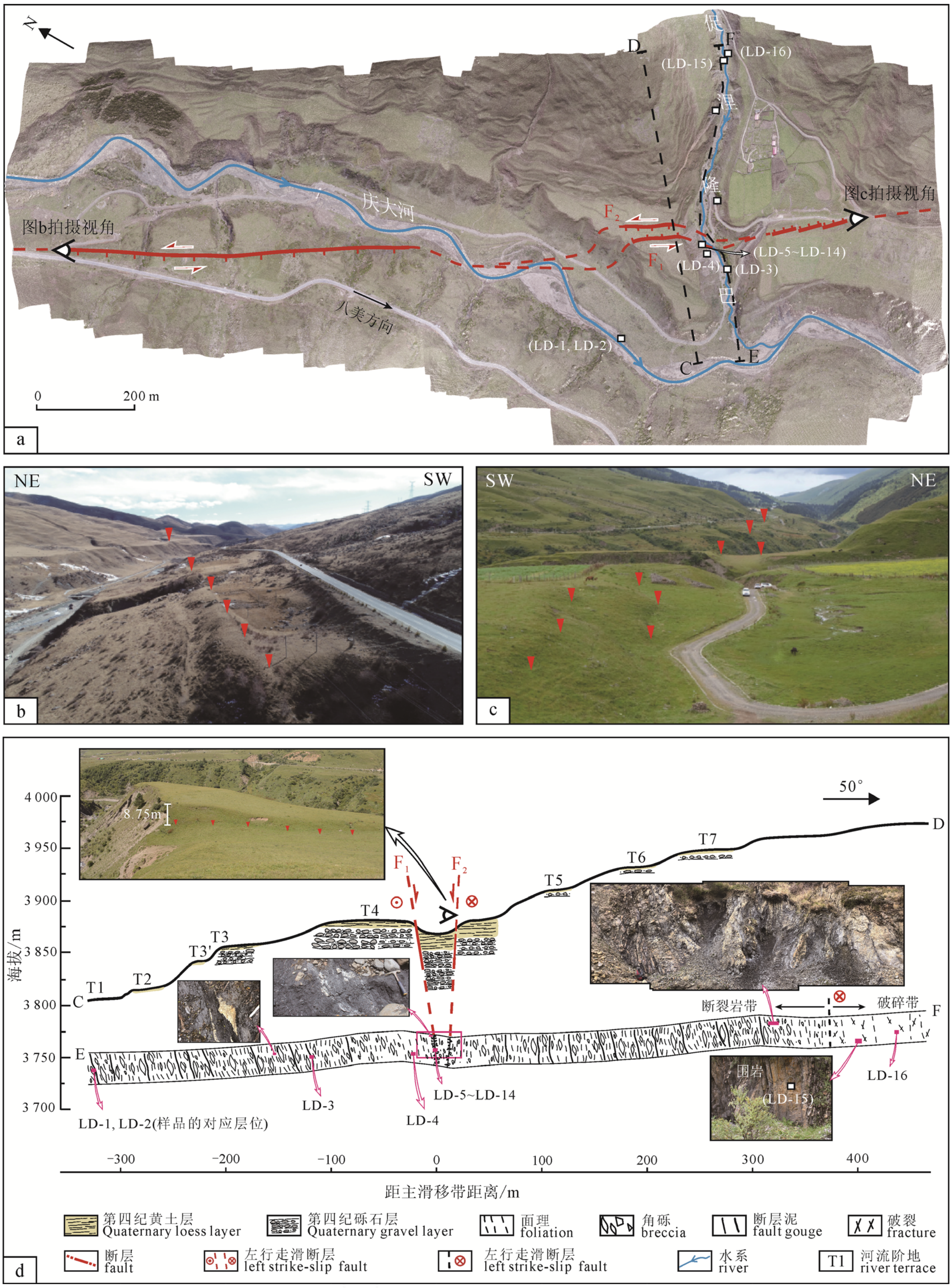


a—无人机合成的数字高程模型图，红色为断裂行迹，蓝色线条为河流及流向，白色方块表示采样点位置；b、c—断层陡坎野外照片，拍摄位置见图 a，红色箭头指示了断层位置；d—促涅隆巴河沟出露的断裂岩剖面，T1~T7 表示河流阶地。

a–unmanned aerial vehicle (UAV) orthorectified image of the Longdeng site, with red lines highlighting fault traces, blue lines showing rivers and their flow directions, and white squares are sample locations; b, c–field photos showing fault scarps, with locations shown in Fig. a and red arrows showing the locations of the fault zone; d–fault rock profile along the Gunielongba River, with T1–T7 representing the various terraces.

**图 7　鲜水河断裂带乾宁段构造地貌特征及促涅隆巴河沟出露的断裂岩剖面(吴琼等, 2023)**

**Fig. 7　Geomorphological features and section of the fault rock in the Qianning segment of the Xianshuihe fault zone (WU et al., 2023)**

入脉和被截切的石英脉等结构构造。这些现象表明乾宁段在蠕滑变形过程中存在地震黏滑变形行为。

## 2.2　鲜水河断裂带局部强化新机制

断裂岩的组成和不均一性决定了断层强度，而断层强度控制了断层摩擦稳定性(Bedford et al., 2022)。研究表明含有大量石英、长石、橄榄石和方解石等强矿物的断裂带通常具有大摩擦系数(0.6~0.85)，其断裂岩一般表现出黏滑或者不稳定

滑动的速度弱化变形行为(Di Toro et al., 2005; Volpe et al., 2022)。而富含绿泥石、滑石、白云母、利蛇纹石和纤维蛇纹石等弱矿物(黏土矿物)的断裂岩具有比较低的摩擦系数(0.1~0.3)，通常更倾向于发生蠕滑或者稳定滑动的速度强化的变形(Tesei et al., 2015; Collettini et al., 2019)。因此，断裂岩中强弱矿物的占比可在一定程度上控制断层的变形行为。

蠕滑变形形成的断裂岩中黏土矿物含量略高于围岩，而强矿物含量明显低于围岩，原因是断裂岩中长石和白云母在流体作用下蚀变为黏土矿物，并定向排列在角砾周围或者聚集在密集的面理内(吴琼等, 2023)。流体作用降低了强矿物含量，弱化了断层，促进了断层浅部的蠕滑变形。然而，长期蠕滑变形的鲜水河断裂带乾宁段内由地震滑动形成的主滑移带断层泥和其两侧断层角砾岩内强矿物总含量远高于弱矿物含量(图 8)，也高于蠕滑变形的断裂岩中强矿物含量，尤其是碳酸盐矿物含量异常高，这是由于富含幔源和热变质脱碳来源 $CO_2$ 的深部热液在震后阶段沿地震产生的破裂上涌至断裂带核部，造成了强烈的水岩反应和广泛的碳酸盐矿物沉淀(图 8)。

传统观点认为地下流体一般会在震后阶段通过水岩反应将断裂带内石英、长石等强矿物蚀变成伊利石和绿泥石等弱矿物，使断层变弱，进而更易发生蠕滑变形(Collettini et al., 2019)。Wu et al.(2023)和吴琼等(2023)创新性提出流体的注入明显提升断层核部强矿物含量，促进了蠕滑断层的局部变强，改变了“流体可使断层变弱”的传统认识。该研究突破了传统观点，认为在一定条件下流体作用也能导致断层局部变强，使其应力不完全释放或局部闭锁，促进了蠕滑断层在浅部(4 km 以上)的应力累积和地震破裂。这一研究成果不仅为断裂带流体作用研究提供了新的视角，同时也加深了对蠕滑断层地震机制的理解和认识。

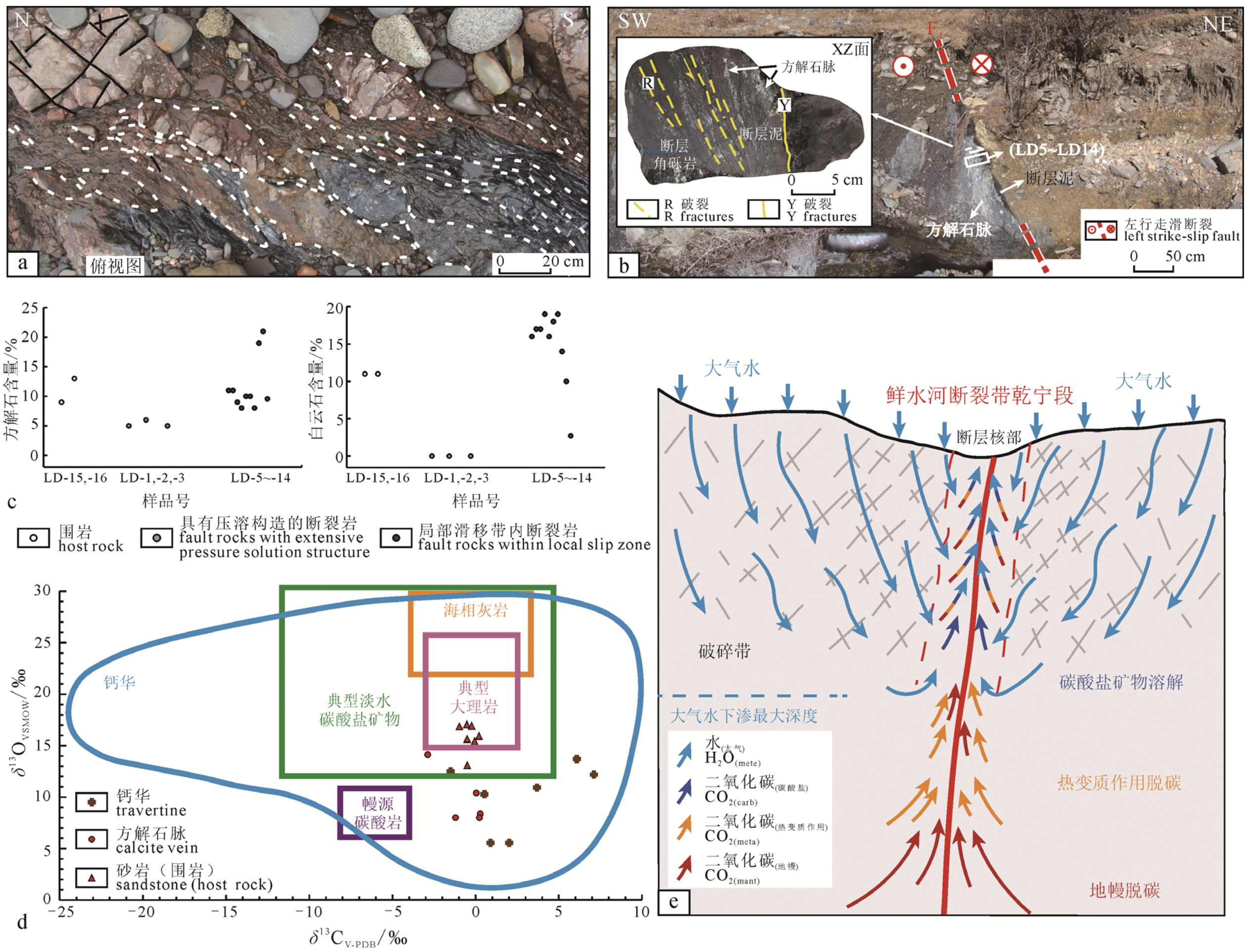


a—乾宁段断裂岩内可见压溶构造广泛发育; b—乾宁段局部滑动带地表露头及主滑移带断裂岩; c—乾宁段砂岩围岩和断裂岩样品内方解石和白云石的相对含量; d—乾宁段主滑移带附近样品的碳氧同位素特征; e—鲜水河断裂带深部热液来源及运移的概念模型。

a–fault breccias showing extensive pressure solution structure within fault rocks along the Qianning segment; b–outcrop of fault slip zone and fault rocks; c–calcite and dolomite content analysis of samples from host and fault rocks along the Qianning segment; d–oxygen and carbon isotope data of samples from the main slip zone in the Qianning segment; e–conceptual model illustrating the source and migration of hydrothermal fluids in the Xianshuihe fault.

**图 8　鲜水河断裂带乾宁段断裂岩结构构造、矿物组成及地下流体来源(Wu et al., 2023)**

**Fig. 8　Structural and mineralogical composition of fault rocks and sources of subsurface fluids in the Qianning segment of the Xianshuihe fault zone (Wu et al., 2023)**

## 3　龙门山断裂带和鲜水河断裂带变形机制的对比分析

映秀—北川断裂带和汶川—茂县断裂带是具有右行走滑性质的逆冲断裂带，而灌县—安县断裂带是逆冲型断裂带(李勇等, 2006; Hubbard et al., 2009; Li et al., 2014; Ge et al., 2023)。映秀—北川断裂带和汶川—茂县断裂带在晚三叠世是具左行走滑性质的断裂带(Ge et al., 2023; Zhang et al., 2024)，持续地震活动从晚三叠世左行走滑转变为新生代右行走滑。北西—南东走向的鲜水河断裂带为左行走滑断裂带(闻学泽等, 1989; Klinger, 2010; Zielke et al., 2015)。Yang et al.(2024)通过全新的贝叶斯算法计算了青藏高原东南缘应变率场(图 9)。通过最大剪切应变率揭示鲜水河—小江断裂系是藏东南物质外迁的主要边界，表明藏东物质是围绕喜马拉雅山东部旋转，并非沿着固定通道整体挤出。在模拟系统的东北和西南地区可见明显的扩张速率模式，例如以龙门山地区为代表的东北地区呈现负扩张异常，而西南地区的金沙江则是呈现正扩张异常。龙门山断裂带和鲜水河断裂带的运动性质不同，且数值模拟结果表明两者的应变率场特征有很大差异(图 9)，可能是由于青藏高原物质沿鲜水河断裂带向东南挤出，同时青藏高原不存在下地壳隧道流模式，龙门山的

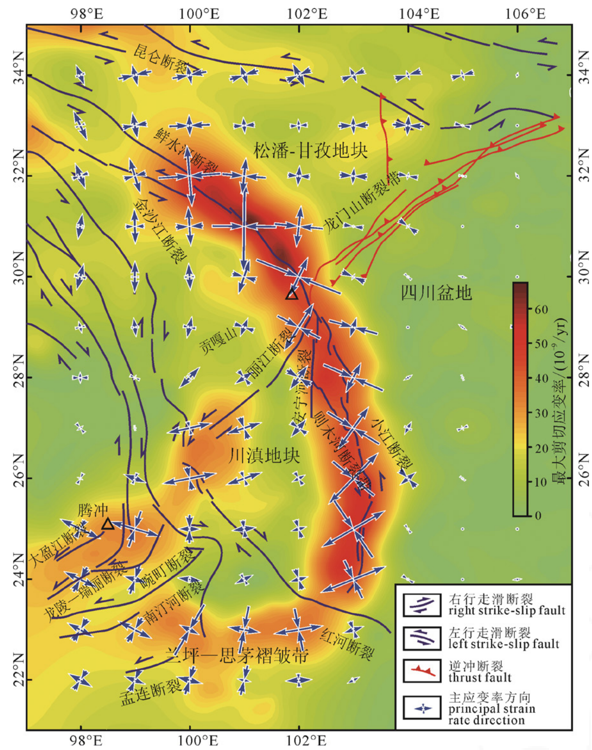


**图 9　基于新开发的贝叶斯算法得出的青藏高原东南缘最大剪切应变速率和主应变速率(Yang et al., 2024)**

**Fig. 9　Maximum shear strain rates and principal strain rates in the southeastern Tibetan Plateau based on a newly developed ABIC method (Yang et al., 2024)**

形成是地壳水平缩短增厚的结果。

龙门山断裂带断裂岩带宽度从数十米到~300 m，主要包括厚层的断层角砾岩和断层泥，同时映秀—北川断裂带存在多组假玄武玻璃(Li et al., 2013, 2016; Wang et al., 2014, 2015, 2019a, b; Zhang et al., 2017; He et al., 2018; 张蕾等, 2023)；而鲜水河断裂带断裂岩宽度高达 700 m，断裂岩带包括断层角砾岩和呈弥散性分布的薄层断层泥(吴琼等, 2023)。龙门山断裂带和鲜水河断裂带中含多层断裂岩带与它们曾经经历频繁的地震活动有关。

龙门山断裂带汶川—茂县断裂带曾经发生过摩擦热温度>500 ℃大地震活动，其孕震和发震环境为含有硫化物的还原性环境(张蕾等, 2023)。映秀—北川断裂带是一条经常发生大地震的黏滑型断裂带(Li et al., 2013; Wang et al., 2014, 2019a; Zhang et al., 2017)，其在浅地表到 15 km 深度处的不同位置均形成了假玄武玻璃脉体(Wang et al., 2015, 2023; Zhang et al., 2017)，脉体中的石英部分熔融及单质铁指示了其经历的摩擦热温度高达 1 300 ℃以上(Zhang et al., 2018; 张蕾等, 2019)，脉体的岩石磁学和结构特征揭示了映秀—北川断裂带深部弱流体作用的还原性孕震环境(张蕾等, 2018)。灌县—安县断裂带是一条不经常发生大地震的蠕滑型断裂带(He et al., 2018; 何祥丽等, 2018)，目前尚未有假玄武玻璃的报道；断裂带的岩石磁学、结构和地球化学成分的研究揭示了其断裂作用环境是低温(<300 ℃)还原性的环境，伴随强流体作用(Liu et al., 2014; He et al., 2018; 何祥丽等, 2018)。龙门山断裂带的三条主要断裂带的断裂作用环境以还原性为主；汶川—茂县断裂带和灌县—安县断裂带的流体作用较强；汶川—茂县断裂带和映秀—北川断裂带曾经发生了多次大地震活动，而灌县—安县断裂带不经常发生大地震。相关研究表明鲜水河断裂带与灌县—安县断裂带相似，是一条蠕滑型断裂带(Li et al., 2021; Qiao et al., 2021, 2022)。然而，不同的是鲜水河断裂带是强震频发的断裂带，且发震周期较短(国家地震局震害防御司, 1995; 中国地震局震害防御司, 1999; USGS, 2020; 吴琼等, 2021, 2023)。Wu et al.(2023)和吴琼等(2023)认为流体作用导致断层局部变强，使其应力不完全释放或局部闭锁，促进了蠕滑断层在浅部(4 km 以上)的应力累积和地震破裂。鲜水河断裂带伴随有长期的强流体作用。鲜水河断裂带经常发生强地震活动，经历了摩擦热高温，然而却鲜有假玄武玻璃的报道，一方面可能是因为大量同震流体减小了有效正应力，抑制了摩擦热升高，阻碍了摩擦熔体的生成；另一方面可能是因为生成的假玄武玻璃在震后强流体作用下发生蚀变。

## 4 存在问题及未来研究方向

青藏高原东缘的龙门山断裂带和鲜水河断裂带是世界上陆内变形最强烈的地区之一，具有全球最陡的地貌、最频发的地震活动以及最严重的地质灾害。龙门山断裂带和鲜水河断裂带的变形机制对于认识大陆内部地震发生机制具有重要意义。目前已经结合地质学、地球物理学、岩石磁学、地球化学、年代学及实验模拟等多学科方法，在龙门山断裂带和鲜水河断裂带的孕震环境、断裂活动性质、以及它们在不同地质时期的演化等方面取得了重要的进展与突破。然而，龙门山断裂带和鲜水河断裂带经过了多期次的构造演化，断裂系统复杂，具有不同类型和活动性质的断裂，局部孕震环境变化和差异较大，断裂带精细结构不够清楚，仍然存在如下主要问题:

(1)龙门山断裂带中的汶川—茂县断裂带在2008年汶川地震中为什么不发生破裂？然而，同时发生破裂的映秀—北川断裂带和灌县—安县断裂带为什么具有不同的长期变形行为和断裂作用环境？

(2)鲜水河断裂带和灌县—安县断裂带均具有长期蠕滑特征，为什么鲜水河断裂带会频繁发生大地震活动？断裂带的蠕滑行为与黏滑行为的转变机制尚不明确。

(3)鲜水河断裂带和映秀—北川断裂带均是长期发生大地震的断裂带，为什么鲜水河断裂带上没有发现大量的摩擦熔融作用？需要进一步确定流体对断裂带变形行为和精细结构的影响。

这些问题制约着龙门山断裂带和鲜水河断裂带变形机制的研究，同时制约着强震发生规律和发生机制的研究。龙门山断裂带和鲜水河断裂带未来研究方向在于: (1)通过野外调查、实验、数值模拟和人工智能等技术方法，联合多领域、多学科开展断裂带的精细结构、物性特征和化学成分等研究，确定同一断裂带不同位置和不同深度的变形机制，对比分析不同断裂带的变形机制。(2)确定并长期观测断裂带不同位置和深度的应力分布状态，分析大地震后(龙门山断裂带)和大地震前(鲜水河断裂带)的应力分布状态对断裂带的变形行为和强震发生规律的控制作用。

## 5 结论

通过以上研究，我们对青藏高原东缘龙门山断裂带和鲜水河断裂带的变形机制有了如下认识:

(1)在 WFSD-1 钻孔 732.6 m 深处断层泥中发现了汶川地震形成的假玄武玻璃，这是首次发现大地震活动在地壳浅部富流体断层泥中发生了熔融作用，补充完善了地震的传统认识，深化了对浅层断层力学过程的认识。大地震可以沿多个不同运动性质的分支断裂同时破裂，且在不同深度伴有不同的滑移机制。

(2)龙门山断裂带映秀—北川断裂带在晚三叠世曾经发生了逆冲-左行走滑的大地震活动，首次提出断裂岩高磁化率各向异性度值指示了强应变环境的大地震活动，补充了地震断裂岩的岩石磁学理论。

(3)龙门山断裂带汶川—茂县断裂带在新生代存在三期构造变形阶段，青藏高原不存在下地壳隧道流机制，为强震背景和山脉隆升机制提供了新证据。首次揭示了汶川—茂县断裂带曾发生摩擦热温度>500 ℃的大地震活动，孕震环境为还原性含硫化物的低温热液流体环境。

(4)强震频发的鲜水河断裂带是藏东南物质外迁的主要边界，具有长期蠕滑变形行为，伴随有强流体作用，地下流体作用能够局部强化断层，并诱发地震，提出了断裂强化过程与诱发地震的新机制，改变了传统观点。

**致谢:** 审稿专家北京大学张波副教授及《地球学报》编辑马铭株博士对本文提出了宝贵的修改意见，提升了本文的质量，在此一并表示感谢!

## Acknowledgements

This study was supported by the National Natural Science Foundation of China (Nos. 42230312, 42172262, 42372266, 42072240, 42020104007, 42272270, and 42374121), the Fundamental Research Funds of the Chinese Academy of Geological Sciences (No. J2403), and the China Geological Survey (No. DD20221630).

## 参考文献:

国家地震局震害防御司, 1995. 中国历史强震目录: 公元前 23 世纪—公元 1911 年[M]. 北京: 地震出版社.

何祥丽, 李海兵, 张蕾, 等, 2018. 龙门山灌县—安县断裂带断层泥低磁化率的矿物、化学响应和蠕滑作用环境[J]. 地球物理学报, 61(5): 1782-1796.

李海兵, 王宗秀, 付小方, 等, 2008. 2008 年 5 月 12 日汶川地震(Ms8.0) 地表破裂带的分布特征[J]. 中国地质, 35(5): 803-813.

李勇, 黄润秋, DENSMORE A L, 等, 2009. 龙门山小鱼洞断裂在汶川地震中的地表破裂及地质意义[J]. 第四纪研究, 29(3): 502-512.

李勇, 周荣军, DENSMORE A L, 等, 2006. 青藏高原东缘龙门山晚新生代走滑-逆冲作用的地貌标志[J]. 第四纪研究, 26(1): 40-51.

罗良, 贾东, 陈竹新, 等, 2006. 川西北磁组构演化及其揭示的应变特征[J]. 地质通报, 25(11): 1342-1348.

罗良, 贾东, 李一泉, 等, 2008. 构造叠加弱应变沉积岩地区的磁组构研究——以川西北盆地为例[J]. 地质学报, 82(6): 850-856.

罗良, 漆家福, 贾东, 等, 2013. 龙门山南段山前天全—乐山剖面磁组构研究及其对新生代构造变形的指示意义[J]. 地球物理学报, 56(2): 558-566.

潘家伟, 李海兵, CHEVALIER M L, 等, 2020. 鲜水河断裂带色

拉哈—康定段新发现的活动断层: 木格措南断裂[J]. 地质学报, 94(11): 3178-3188.
王二七, 孟庆任, 2008. 对龙门山中生代和新生代构造演化的讨论[J]. 中国科学(D 辑: 地球科学), 38(10): 1221-1233.
王焕, 李海兵, 司家亮, 等, 2023. 汶川地震假玄武玻璃的特征、成因及其构造意义[J]. 岩石学报, 39(12): 3833-3847.
闻学泽, 2000. 四川西部鲜水河-安宁河-则木河断裂带的地震破裂分段特征[J]. 地震地质, 22(3): 239-249.
闻学泽, ALLEN C R, 罗灼礼, 等, 1989. 鲜水河全新世断裂带的分段性、几何特征及其地震构造意义[J]. 地震学报, 11(4): 362-372.
吴琼, 李海兵, CHEVALIER M L, 等, 2021. 鲜水河断裂带乾宁段岩石特征与内部结构及其物理-化学性质[J]. 岩石学报, 37(10): 3204-3224.
吴琼, 李海兵, CHEVALIER M L, 等, 2023. 鲜水河断裂带乾宁段蠕滑变形及局部粘滑变形的岩石学记录[J]. 岩石学报, 39(12): 3797-3816.
徐晶, 邵志刚, 马宏生, 等, 2013. 鲜水河断裂带库仑应力演化与强震间关系[J]. 地球物理学报, 56(4): 1146-1158.
徐锡伟, 闻学泽, 叶建青, 等, 2008. 汶川 Ms8.0 地震地表破裂带及其发震构造[J]. 地震地质, 30(3): 597-629.
许志琴, 李海兵, 吴忠良, 2008. 汶川地震和科学钻探[J]. 地质学报, 82(12): 1613-1622.
张蕾, 李海兵, 孙知明, 等, 2019. 断裂熔融作用中单质铁的形成及其指示的孕震环境[J]. 岩石学报, 35(6): 1875-1891.
张蕾, 李海兵, 孙知明, 等, 2023. 龙门山汶川-茂县断裂带的岩石磁学特征及其地震作用的指示意义[J]. 岩石学报, 39(12): 3817-3832.
张蕾, 李海兵, 孙知明, 等, 2018. 龙门山断裂带大地震孕震环境的岩石磁学证据[J]. 地球物理学报, 61(5): 1715-1727.
张培震, 徐锡伟, 闻学泽, 等, 2008. 2008 年汶川 8.0 级地震发震断裂的滑动速率、复发周期和构造成因[J]. 地球物理学报, 51(4): 1066-1073.
中国地震局震害防御司, 1999. 中国近代地震目录: 公元 1912 年~1990 年, Ms≥4.7[M]. 北京: 中国科学技术出版社.

## References:

ADAMS B A, HODGES K V, 2022. Potential influences of middle and lower crustal flow on landscape evolution: insights from the Himalayan-Tibetan Orogen[M]//SHRODER J F. Treatise on Geomorphology. Amsterdam: Elsevier: 729-748.
ALLEN C R, LUO Zhouli, QIAN Hong, et al., 1991. Field study of a highly active fault zone: The Xianshuihe fault of southwestern China[J]. Geological Society of America Bulletin, 103(9): 1178-1199.
ANDERSEN T B, AUSTRHEIM H, 2006. Fossil earthquakes recorded by pseudotachylytes in mantle peridotite from the Alpine subduction complex of Corsica[J]. Earth and Planetary Science Letters, 242(1-2): 58-72.
ANDREWS D J, 2002. A fault constitutive relation accounting for thermal pressurization of pore fluid[J]. Journal of Geophysical Research: Solid Earth, 107(B12): 2363.
BAI Mingkun, CHEVALIER M L, LELOUP P H, et al., 2021. Spatial slip rate distribution along the SE Xianshuihe Fault, Eastern Tibet, and earthquake hazard assessment[J]. Tectonics, 40(11): e2021TC006985.
BAI Mingkun, CHEVALIER M L, PAN Jiawei, et al., 2018. Southeastward increase of the late Quaternary slip-rate of the Xianshuihe fault, eastern Tibet. Geodynamic and seismic hazard implications[J]. Earth and Planetary Science Letters, 485: 19-31.
BARKER S L L, 2005. Pseudotachylyte-generating faults in Central Otago, New Zealand[J]. Tectonophysics, 397(3-4): 211-223.
BEDFORD J D, FAULKNER D R, LAPUSTA N, 2022. Fault rock heterogeneity can produce fault weakness and reduce fault stability[J]. Nature Communications, 13: 326.
BOULLIER A M, OHTANI T, FUJIMOTO K, et al., 2001. Fluid inclusions in pseudotachylytes from the Nojima Fault, Japan[J]. Journal of Geophysical Research: Solid Earth, 106(B10): 21965-21977.
BRANTUT N, SCHUBNEL A, CORVISIER J, et al., 2010. Thermochemical pressurization of faults during coseismic slip[J]. Journal of Geophysical Research: Solid Earth, 115(B5): B05314.
BURCHFIEL B C, ROYDEN L H, VAN DER HILST R D, et al., 2008. A geological and geophysical context for the Wenchuan earthquake of 12 May 2008, Sichuan, People's Republic of China[J]. GSA Today, 18(7): 4-11.
CHEN K H, BÜRGMANN R, 2017. Creeping faults: Good news, bad news?[J]. Reviews of Geophysics, 55(2): 282-286.
CHENG Jia, LIU Jie, GAN Weijun, et al., 2011. Characteristics of strong earthquake evolution around the eastern boundary faults of the Sichuan-Yunnan rhombic block[J]. Science China Earth Sciences, 54(11): 1716-1729.
CHOU Yumin, AUBOURG C, YEH E C, et al., 2020. The magnetic fabric of gouge mimics the coseismic focal mechanism of the chi-chi earthquake (1999, Mw 7.6)[J]. Geophysical Research Letters, 47: e2020GL090111.
CHOU Yumin, SONE Shengrong, AUBOURG C, et al., 2012. An earthquake slip zone is a magnetic recorder[J]. Geology, 40(6): 551-554.
COLLETTINI C, TESEI T, SCUDERI M M, et al., 2019. Beyond Byerlee friction, weak faults and implications for slip behavior[J]. Earth and Planetary Science Letters, 519: 245-263.
COWAN D S, 1999. Do faults preserve a record of seismic slip? A field geologist's opinion[J]. Journal of Structural Geology, 21(8-9): 995-1001.
DI TORO G, PENNACCHIONI G, 2005. Fault plane processes and mesoscopic structure of a strong-type seismogenic fault in tonalites (Adamello batholith, Southern Alps)[J]. Tectonophysics, 402(1-4): 55-80.
DI TORO G, PENNACCHIONI G, NIELSEN S, 2009. Pseudotachylytes and earthquake source mechanics[M]// International Geophysics. Amsterdam: Elsevier: 87-133.
Earthquake Disaster Prevention Department of State Seismological Bureau, 1995. Catalogue of Chinese Historical Strong Earthquakes (23rd century B.C. to 1911 A.D.)[M]. Beijing: Seismological Press(in Chinese with English Summery).
Earthquake Disaster Prevention Department of the China Earthquake Administration, 1999. Catalogue of Chinese Earthquakes (1912~1990, $M_S$≥4.77)[M]. Beijing: China Science and Technology Press(in Chinese with English Summery).
FERRÉ E C, CHOU Youmin, KUO R L, et al., 2016. Deciphering viscous flow of frictional melts with the mini-AMS method[J]. Journal of Structural Geology, 90: 15-26.
FERRÉ E C, GEISSMAN J W, CHAUVET A, et al., 2015. Focal mechanism of prehistoric earthquakes deduced from pseudotachylyte fabric[J]. Geology, 43(6): 531-534.

FERRÉ E C, GEISSMAN J W, ZECHMEISTER M S, 2012. Magnetic properties of fault pseudotachylytes in granites[J]. Journal of Geophysical Research: Solid Earth, 117: B01106.

FIALKO Y, KHAZAN Y, 2005. Fusion by earthquake fault friction: Stick or slip?[J]. Journal of Geophysical Research: Solid Earth, 110(B12): B12407.

FONDRIEST M, MECKLENBURGH J, PASSELEGUE F X, et al., 2020. Pseudotachylyte alteration and the rapid fade of earthquake scars from the geological record[J]. Geophysical Research Letters, 47(22): 749-761.

FU Bihong, SHI Pilong, GUO Huadong, et al., 2011. Surface deformation related to the 2008 Wenchuan earthquake, and mountain building of the Longmen Shan, eastern Tibetan Plateau[J]. Journal of Asian Earth Sciences, 40(4): 805-824.

GE Chenglong, LELOUP P H, ZHENG Yong, et al., 2023. Cenozoic kinematics of the Wenchuan-Maoxian fault implies crustal stacking rather than channel flow extrusion at the eastern margin of Tibetan plateau (Longmen Shan)[J]. Tectonophysics, 857: 229816.

GRATIER J P, THOUVENOT F, JENATTON L, et al., 2013. Geological control of the partitioning between seismic and aseismic sliding behaviours in active faults: Evidence from the Western Alps, France[J]. Tectonophysics, 600: 226-242.

GUO Rumeng, ZHENG Yong, TIAN Wen, et al., 2018. Locking status and earthquake potential hazard along the middle-south Xianshuihe fault[J]. Remote Sensing, 10(12): 2048.

HARRIS R A, 2017. Large earthquakes and creeping faults[J]. Reviews of Geophysics, 55(1): 169-198.

HE Xiangli, LI Haibing, WANG Huan, et al., 2018. Creeping along the Guanxian-Anxian fault of the 2008 Mw 7.9 Wenchuan earthquake in the Longmen Shan, China[J]. Tectonics, 37(7): 2124-2141.

HE Xiangli, LI Haibing, ZHANG Lei, et al., 2018. Mineral and chemical response to low magnetic susceptibility of the fault gouge from the Guanxian-Anxian fault zone and fault creep setting in the Longmen Shan[J]. Chinese Journal of Geophysics, 61(5): 1782-1796(in Chinese with English abstract).

HIRONO T, IKEHARA M, OTSUKI K, et al., 2006. Evidence of frictional melting from disk-shaped black material, discovered within the Taiwan Chelungpu fault system[J]. Geophysical Research Letters, 33: L19311.

HOUSEN B A, VAN DER PLUIJM B A, ESSENE E J, 1995. Plastic behavior of magnetite and high strains obtained from magnetic fabrics in the Parry Sound shear zone, Ontario Grenville Province[J]. Journal of Structural Geology, 17(2): 265-278.

HUBBARD J, SHAW J H, 2009. Uplift of the Longmen Shan and Tibetan Plateau, and the 2008 Wenchuan (M=7.9) earthquake[J]. Nature, 458(7235): 194-197.

HUBBARD J, SHAW J H, KLINGER Y, 2010. Structural setting of the 2008 Mw 7.9 Wenchuan, China, earthquake[J]. Bulletin of the Seismological Society of America, 100(5B): 2713-2735.

JAYANGONDAPERUMAL R, DUBEY A K, SENTHIL KUMAR B, et al., 2010. Magnetic fabrics indicating Late Quaternary seismicity in the Himalayan foothills[J]. International Journal of Earth Sciences, 99(S1): S265-S278.

JIA Dong, LI Yiquan, LIN Aiming, et al., 2010. Structural model of 2008 Mw 7.9 Wenchuan earthquake in the rejuvenated Longmen Shan thrust belt, China[J]. Tectonophysics, 491: 174-184.

JIANG Guoyan, XU Xiwei, CHEN Guihua, et al., 2015. Geodetic imaging of potential seismogenic asperities on the Xianshuihe-Anninghe-Zemuhe fault system, Southwest China, with a new 3-D viscoelastic interseismic coupling model[J]. Journal of Geophysical Research: Solid Earth, 120(3): 1855-1873.

KIRKPATRICK J D, ROWE C D, 2013. Disappearing ink: How pseudotachylytes are lost from the rock record[J]. Journal of Structural Geology, 52: 183-198.

KIRKPATRICK J D, DOBSON K J, MARK D F, et al., 2012. The depth of pseudotachylyte formation from detailed thermochronology and constraints on coseismic stress drop variability[J]. Journal of Geophysical Research: Solid Earth, 117: B06406.

KLEMPERER S L, 2006. Crustal flow in Tibet: Geophysical evidence for the physical state of Tibetan lithosphere, and inferred patterns of active flow[J]. Geological Society of London Special Publication, 268(1): 39-70.

KLINGER Y, 2010. Relation between continental strike-slip earthquake segmentation and thickness of the crust[J]. Journal of Geophysical Research: Solid Earth, 115: B07306.

KONTNY A, ENGELMANN R, GRIMMER J C, et al., 2012. Magnetic fabric development in a highly anisotropic magnetite-bearing ductile shear zone (Seve Nappe Complex, Scandinavian Caledonides)[J]. International Journal of Earth Sciences, 101(3): 671-692.

LEVI T, WEINBERGER R, AÏFA T, et al., 2006. Earthquake-induced clastic dikes detected by anisotropy of magnetic susceptibility[J]. Geology, 34(2): 69-72.

LI Haibing, WANG Huan, XU Zhiqin, et al., 2013. Characteristics of the fault-related rocks, fault zones and the principal slip zone in the Wenchuan Earthquake Fault Scientific Drilling Project Hole-1 (WFSD-1)[J]. Tectonophysics, 584: 23-42.

LI Haibing, WANG Huan, YANG Guang, et al., 2016. Lithological and structural characterization of the Longmen Shan fault belt from the 3rd hole of the Wenchuan Earthquake Fault Scientific Drilling project (WFSD-3)[J]. International Journal of Earth Sciences, 105(8): 2253-2272.

LI Haibing, WANG Zongxiu, FU Xiaofang, et al., 2008. The surface rupture zone distribution of the Wenchuan earthquake (Ms 8.0) happened on May 12th, 2008[J]. Geology in China, 35(5): 803-813(in Chinese with English abstract).

LI Haibing, XU Zhiqin, NIU Yixiong, et al., 2014. Structural and physical property characterization in the Wenchuan Earthquake Fault Scientific Drilling Project-Hole 1 (WFSD-1)[J]. Tectonophysics, 619-620: 86-100.

LI Yiquan, JIA Dong, LUO Liang, et al., 2007. Three dimension construction and magnetic fabric analysis of the Yanjinggou fault-propagation fold in western Sichuan[J]. Earth Science Frontiers, 14(4): 74-84.

LI Yong, HUANG Runqiu, DENSMORE A L, et al., 2009. Surface rupture of Xiaoyudong fault caused by Wenchuan earthquake and its geological significance[J]. Quaternary Sciences, 29(3): 502-512(in Chinese with English abstract).

LI Yong, ZHOU Rongjun, DENSMORE A L, et al., 2006. Geomorphic evidence for the Late Cenozoic strike-slipping and thrusting in Longmen Mountain at the eastern margin of the Tibetan Plateau[J]. Quaternary Sciences, 26(1): 40-51(in Chinese with English abstract).

LI Yuexin, BÜRGMANN R, 2021. Partial coupling and earthquake potential along the Xianshuihe fault, China[J]. Journal of Geophysical Research: Solid Earth, 126(7): e2020JB021406.

LIN Aiming, 2008. Fossil Earthquakes: The Formation and Preservation of Pseudotachylites[M]. Berlin: Springer.

LIU Dongliang, LI Haibing, LEE T Q, et al., 2014. Primary rock magnetism for the Wenchuan earthquake fault zone at Jiulong outcrop, Sichuan Province, China[J]. Tectonophysics, 619-620: 58-69.

LU Renqi, HE Dengfa, XU Xiwei, et al., 2016. Crustal-scale tectonic wedging in the central Longmen Shan: Constraints on the uplift mechanism in the southeastern margin of the Tibetan Plateau[J]. Journal of Asian Earth Sciences, 117: 73-81.

LUO Liang, JIA Dong, CHEN Zhuxin, et al., 2006. Magnetic fabric evolution in the northwestern Sichuan basin, China and its strain characteristics[J]. Geological Bulletin of China, 25(11): 1342-1348(in Chinese with English abstract).

LUO Liang, JIA Dong, LI Yiquan, et al., 2008. Magnetic fabric of weak deformed sediments under the tectonic superposition: A case of the Northwest Sichuan Basin[J]. Acta Geologica Sinica, 82(6): 850-856(in Chinese with English abstract).

LUO Liang, QI Jiafu, JIA Dong, et al., 2013. Magnetic fabric investigation in Tianquan-Leshan section in front of Longmenshan fold-thrust belt and its indicative significance for the Cenozoic deformation[J]. Chinese Journal of Geophysics, 56(2): 558-566(in Chinese with English abstract).

LUO Liang, QI Jiafu, ZHANG Mingzheng, 2014. AMS investigation in the Pingluoba and Qiongxi anticlines, Sichuan, China: Implications for deformation mechanism of the Qiongxi structure[J]. Tectonophysics, 626: 186-196.

MADDOCK R H, GROCOTT J, VAN NES M, 1987. Vesicles, amygdales and similar structures in fault-generated pseudotachylytes[J]. Lithos, 20(5): 419-432.

MERZ L, ALMQVIST B S G, GRIMMER J C, et al., 2019. Magnetic fabric development in the Lower Seve thrust from the COSC-1 drilling, Swedish Caledonides[J]. Tectonophysics, 751: 212-228.

MISHIMA T, HIRONO T, NAKAMURA N, et al., 2009. Changes to magnetic minerals caused by frictional heating during the 1999 Taiwan Chi-Chi earthquake[J]. Earth Planets Space, 61(6): 797-801.

MITTEMPERGHER S, DALLAI L, PENNACCHIONI G, et al., 2014. Origin of hydrous fluids at seismogenic depth: Constraints from natural and experimental fault rocks[J]. Earth and Planetary Science Letters, 385: 97-109.

PAN Jiawei, LI Haibing, CHEVALIAR M L, et al., 2020. A newly discovered active fault on the Selaha-Kangding segment along the SE Xianshuihe fault: the South Mugecuo fault[J]. Acta Geologica Sinica, 94(11): 3178-3188.

QIAO Xin, ZHOU Yu, ZHANG Peizhen, 2022. Along-strike variation in fault structural maturity and seismic moment deficits on the Yushu-Ganzi-Xianshuihe fault system revealed by strain accumulation and regional seismicity[J]. Earth and Planetary Science Letters, 596: 117799.

QIAO Xin, ZHOU Yu, 2021. Geodetic imaging of shallow creep along the Xianshuihe fault and its frictional properties[J]. Earth and Planetary Science Letters, 567: 117001.

RICE J R, 2006. Heating and weakening of faults during earthquake slip[J]. Journal of Geophysical Research: Solid Earth, 111(B5): B05311.

ROYDEN L H, BURCHFIEL B C, KING R W, et al., 1997. Surface deformation and lower crustal flow in eastern Tibet[J]. Science, 276(5313): 788-790.

ROYDEN L H, BURCHFIEL B C, VAN DER HILST R D, 2008. The geological evolution of the Tibetan Plateau[J]. Science, 321(5892): 1054-1058.

SCHOLZ C H, 1988. The brittle-plastic transition and the depth of seismic faulting[J]. Geologische Rundschau, 77(1): 319-328.

SHAN Bin, XIONG Xiong, ZHENG Yong, et al., 2009. Stress changes on major faults caused by M w7.9 Wenchuan earthquake, May 12, 2008[J]. Science in China Series D: Earth Sciences, 52(5): 593-601.

SHEN Zhengkang, SUN Jianbao, ZHANG Peizhen, et al., 2009. Slip maxima at fault junctions and rupturing of barriers during the 2008 Wenchuan earthquake[J]. Nature Geoscience, 2(10): 718-724.

SIBSON R H, 1975. Generation of pseudotachylyte by ancient seismic faulting[J]. Geophysical Journal International, 43(3): 775-794.

SIBSON R H, 1977. Fault rocks and fault mechanisms[J]. Journal of the Geological Society, 133(3): 191-213.

SIBSON R H, TOY V G, 2006. The habitat of fault-generated pseudotachylyte: Presence vs. absence of friction-melt[M]//Geophysical Monograph Series. Washington D. C.: American Geophysical Union: 153-166.

SIBSON R H, 1983. Continental fault structure and the shallow earthquake source[J]. Journal of the Geological Society, 140(5): 741-767.

TAPPONNIER P, XU Zhiqin, ROGER F, et al., 2001. Oblique stepwise rise and growth of the Tibet Plateau[J]. Science, 294(5547): 1671-1677.

TESEI T, LACROIX B, COLLETTINI C, 2015. Fault strength in thin-skinned tectonic wedges across the smectite-illite transition: Constraints from friction experiments and critical tapers[J]. Geology, 43(10): 923-926.

TIAN Yuntao, KOHN B P, GLEADOW A J W, et al., 2013. Constructing the Longmen Shan eastern Tibetan Plateau margin: Insights from low-temperature thermochronology[J]. Tectonics, 32(3): 576-592.

TODA S, LIN Jian, MEGHRAOUI M, et al., 2008. 12 May 2008 M=7.9 Wenchuan, China, earthquake calculated to increase failure stress and seismicity rate on three major fault systems[J]. Geophysical Research Letters, 35(17): L17305.

USGS. Earthquakes[EB/OL]. [2020-07-20]. https://www.usgs.gov/programs/earthquake-hazards/earthquakes.

VOLPE G, POZZI G, COLLETTINI C, 2022. Y-B-P-R or S-C-C'? Suggestion for the nomenclature of experimental brittle fault fabric in phyllosilicate-granular mixtures[J]. Journal of Structural Geology, 165: 104743.

WANG Erqi, MENG Qingren, 2008. Discussion on the Mesozoic and Cenozoic tectonic evolution of the Longmen Shan fault belt[J]. Science in China (Series D), 38(10): 1221-1233(in Chinese).

WANG Huan, LI Haibing, DI TORO G, et al., 2023. Melting of fault gouge at shallow depth during the 2008 Mw 7.9 Wenchuan earthquake, China[J]. Geology, 51(4): 345-350.

WANG Huan, LI Haibing, JANSSEN C, et al., 2015. Multiple generations of pseudotachylyte in the Wenchuan fault zone and their implications for coseismic weakening[J]. Journal of Structural Geology, 74: 159-171.

WANG Huan, LI Haibing, SI Jialiang, et al., 2014. Internal structure of the Wenchuan earthquake fault zone, revealed by surface outcrop and WFSD-1 drilling core investigation[J]. Tectonophysics, 619-620: 101-114.

WANG Huan, LI Haibing, SI Jialiang, et al., 2019b. Geochemical features of the pseudotachylytes in the Longmen Shan thrust belt, eastern Tibet[J]. Quaternary International, 514: 173-185.

WANG Huan, LI Haibing, SI Jialiang, et al., 2023. Characteristics, genesis and tectonic significance of the pseudotachylyte produced by the Wenchuan earthquake[J]. Acta Petrologica Sinica, 39(12): 3833-3847(in Chinese with English abstract).

WANG Huan, LI Haibing, ZHANG Lei, et al., 2019a. Paleoseismic slip records and uplift of the Longmen Shan, eastern Tibetan Plateau[J]. Tectonics, 38(1): 354-373.

WANG Min, SHEN Zhengkang, 2020. Present-day crustal deformation of continental China derived from GPS and its tectonic implications[J]. Journal of Geophysical Research: Solid Earth, 125(2): e2019JB018774.

WELLS D L, COPPERSMITH K J, 1994. New empirical relationships among magnitude, rupture length, rupture width, rupture area, and surface displacement[J]. Bulletin of the Seismological Society of America, 84(4): 974-1002.

WEN Xueze, 2000. Character of rupture segmentation of the Xianshuihe-Anninghe-Zemuhe fault zone, western Sichuan[J]. Seismology and Geology, 22(3): 239-249(in Chinese with English abstract).

WEN Xueze, ALLEN C R, LUO Zhuoli, et al., 1989. Segmentation, geometric features, and their seismotectonic implications for the Holocene Xianshuihe fault zone[J]. Acta Seismologica Sinica, 11(4): 362-372(in Chinese with English abstract).

WEN Xueze, MA Shengli, XU Xiwei, et al., 2008. Historical pattern and behavior of earthquake ruptures along the eastern boundary of the Sichuan-Yunnan faulted-block, southwestern China[J]. Physics of the Earth and Planetary Interiors, 168: 16-36.

WU Qiong, LI Haibing, CHEVALIER M L, et al., 2023. Fluid influx promotes local strengthening of the creeping Xianshuihe fault, eastern Tibet[J]. Journal of Geophysical Research: Solid Earth, 128(7): e2023JB026682.

WU Qiong, LI Haibing, CHEVALIER M L, et al., 2021. Rock characteristics, internal structure and physical-chemical properties of Qianning segment in Xianshuihe fault zone[J]. Acta Petrologica Sinica, 37(10): 3204-3224(in Chinese with English abstract).

WU Qiong, LI Haibing, CHEVALIER M L, et al., 2023. Petrological records of creeping and locally stick-slip deformation along Qianning segment of Xianshuihe fault[J]. Acta Petrologica Sinica, 39(12): 3797-3816(in Chinese with English abstract).

XU Jing, SHAO Zhigang, MA Hongsheng, et al., 2013. Evolution of Coulomb stress and stress interaction among strong earthquakes along the Xianshuihe fault zone[J]. Chinese Journal of Geophysics, 56(4): 1146-1158(in Chinese with English abstract).

XU Xiwei, WEN Xueze, YE Jianqing, et al., 2008. The Ms8.0 Wenchuan earthquake surface ruptures and its seismogenic structure[J]. Seismology and Geology, 30(3): 597-629(in Chinese with English abstract).

XU Zhiqin, LI Haibing, WU Zhongliang, 2008. Wenchuan earthquake and scientific drilling[J]. Acta Geologica Sinica, 82(12): 1613-1622(in Chinese with English abstract).

YANG Shaohua, PAN Jiawei, LI Haibing, et al., 2024. Present-day upper-crustal strain rate field in southeastern Tibet and its geodynamic implications: Constraints from GPS measurements with ABIC method[J]. Acta Geologica Sinica (English Edition), 98(1): 265-275.

YANG Tao, MISHIMA T, UJIIE K, et al., 2013. Strain decoupling across the décollement in the region of large slip during the 2011 Tohoku-Oki earthquake from anisotropy of magnetic susceptibility[J]. Earth and Planetary Science Letters, 381: 31-38.

YANG Tao, CHOU Yumin, FERRÉ E C, et al., 2020. Faulting processes unveiled by magnetic properties of fault rocks[J]. Reviews of Geophysics, 58(4): e2019RG000690.

YANG Wen, CHENG Jia, LIU Jie, et al., 2015. The Kangding earthquake swarm of November, 2014[J]. Earthquake Science, 28(3): 197-207.

YIN An, HARRISON T M, 2000. Geologic evolution of the Himalayan-Tibetan Orogen[J]. Annual Review of Earth and Planetary Sciences, 28: 211-280.

ZHANG Lei, LI Haibing, FERRÉ E C, et al., 2024. Focal mechanism of a Late Triassic large magnitude earthquake along the Longmen Shan fault belt, eastern Tibetan Plateau[J]. Journal of Structural Geology, 178: 105015.

ZHANG Lei, LI Haibing, SUN Zhiming, et al., 2018. Metallic iron formed by melting: A new mechanism for magnetic highs in pseudotachylyte[J]. Geology, 46(9): 779-782.

ZHANG Lei, LI Haibing, SUN Zhiming, et al., 2018. Rock magnetic evidence for the seismogenic setting of large earthquakes in the Longmen Shan fault zone[J]. Chinese Journal of Geophysics, 61(5): 1715-1727(in Chinese with English abstract).

ZHANG Lei, LI Haibing, SUN Zhiming, et al., 2019. Metallic iron formed by melting and its seismogenic setting indication[J]. Acta Petrologica Sinica, 35(6): 1875-1891(in Chinese with English abstract).

ZHANG Lei, LI Haibing, SUN Zhiming, et al., 2021. Microstructural evolution of pseudotachylyte-bearing rocks during increasing temperatures: Evidence from rock-heating experiments[J]. Journal of Structural Geology, 149: 104398.

ZHANG Lei, LI Haibing, SUN Zhiming, et al., 2023. Rock magnetic characteristics of the Wenchuan-Maoxian fault zone of the Longmen Shan fault and its earthquake faulting characteristics[J]. Acta Petrologica Sinica, 39(12): 3817-3832(in Chinese with English abstract).

ZHANG Lei, SUN Zhiming, LI Haibing, et al., 2017. Rock record and magnetic response to large earthquakes within Wenchuan Earthquake Fault Scientific Drilling cores[J]. Geochemistry, Geophysics, Geosystems, 18(5): 1889-1906.

ZHANG Peizhen, 2013. A review on active tectonics and deep crustal processes of the Western Sichuan region, eastern margin of the Tibetan Plateau[J]. Tectonophysics, 584: 7-22.

ZHANG Peizhen, XU Xiwei, WEN Xueze, et al., 2008. Slip rates and recurrence intervals of the Longmen Shan active fault zone and tectonic implications for the mechanism of the May 12 Wenchuan earthquake, 2008, Sichuan, China[J]. Chinese Journal of Geophysics, 51(4): 1066-1073(in Chinese with English abstract).

ZHENG Yong, LI Haibing, SUN Zhiming, et al., 2016. New geochronology constraints on timing and depth of the ancient earthquakes along the Longmen Shan fault belt, eastern Tibet[J]. Tectonics, 35(12): 2781-2806.

ZHOU Zhicheng, YAN Danping, QIU Liang, et al., 2023. Multi-phase non-coaxial orogenic growth: Propagation of the Longmen Shan thrust belt on the eastern margin of the Tibetan Plateau[J]. Tectonics, 42(9): e2023TC007814.

ZIELKE O, KLINGER Y, ARROWSMITH J R, 2015. Fault slip and earthquake recurrence along strike-slip faults—Contributions of high-resolution geomorphic data[J]. Tectonophysics, 638: 43-62.